THE PROPERTIES OF POOR GROUPS OF GALAXIES:

I. SPECTROSCOPIC SURVEY AND RESULTS

Ann I. Zabludoff[1,2] and John S. Mulchaey[1]

Accepted for publication in *The Astrophysical Journal*

ABSTRACT

We use multi-fiber spectroscopy of 12 poor groups of galaxies to address: (1) whether the groups are bound systems or chance projections of galaxies along the line-of-sight, (2) why the members of each group have not already merged to form a single galaxy, despite the groups' high galaxy densities, short crossing times, and likely environments for galaxy-galaxy mergers, and (3) how galaxies might evolve in these groups, where the collisional effects of the intra-group gas and the tidal influences of the global potential are weaker than in rich clusters. Each of the 12 groups has fewer than $\sim$ five cataloged members in the literature. Our sample consists of 1002 galaxy velocities, 280 of which are group members. The groups have mean recessional velocities between 1600 and 7600 km s^{-1}. Nine groups, including three Hickson compact groups, have the extended X-ray emission characteristic of an intra-group medium (Mulchaey & Zabludoff 1997 (Paper II)).

We conclude the following:

(a) The nine poor groups with diffuse X-ray emission are bound systems with at least $\sim$20-50 group members to $M_B \sim -14$ to $-16 + 5log_{10}\ h$. The large number of group members, the significant early-type population (up to $\sim 55\%$ of the membership) and its concentration in the group center, and the correspondence of the central, giant elliptical with the optical and X-ray group centroids argue that the X-ray groups are not radial superpositions of unbound galaxies. The velocity dispersions of the X-ray groups range from 190 to 460 km s^{-1}. We are unable to determine if the three non-X-ray groups, which have lower velocity dispersions (< 130 km s^{-1}) and early-type fractions ($= 0\%$), are also bound.

(b) Galaxies in each X-ray-detected group have not all merged together, because a significant fraction of the group mass lies outside of the galaxies and in a common halo. The velocity dispersion of the combined group sample is constant as a function of radius out to the virial radius of the system (typically $\sim 0.5h^{-1}$ Mpc). The virial

[1]Observatories of the Carnegie Institution of Washington, 813 Santa Barbara St., Pasadena, CA 91101, E-mail: mulchaey@pegasus.ociw.edu

[2]UCO/Lick Observatory and Board of Astronomy and Astrophysics, University of California at Santa Cruz, Santa Cruz, CA, 95064, E-mail: aiz@ucolick.org

mass of each group ($\sim$ 0.5-1 $\times$ $10^{14}h^{-1}M_{\odot}$) is large compared with the mass in the X-ray gas and in the galaxies (*e.g.*, $\sim 1 \times 10^{12}h^{-5/2}M_{\odot}$ and $\sim 1 \times 10^{13}h^{-1}$ $M_{\odot}$, respectively, in NGC 533). These results imply that most of the group mass is in a common, extended halo. The small fraction ($\sim$ 10-20%) of group mass associated with individual galaxies suggests that the rate of galaxy-galaxy interactions is lower than for a galaxy-dominated system (Governato *et al.* 1991; Bode *et al.* 1993; Athanassoula 1997), allowing these groups to virialize before all of their galaxies merge and to survive for more than a few crossing times.

(c) The position of the giant, brightest elliptical in each X-ray group is indistinguishable from the center of the group potential, as defined by the mean velocity and the projected spatial centroid of the group galaxies. This result suggests that dominant cluster ellipticals, such as "cD" galaxies (Matthews, Morgan, & Schmidt 1965), may form via the merging of galaxies in the centers of poor group-like environments. Groups with a central, dominant elliptical may then fall into richer clusters (Merritt 1985). This scenario explains why "cD"s do not always lie in the spatial and kinematic center of rich clusters (Zabludoff *et al.* 1990; Dunn 1991; Zabludoff *et al.* 1993), but instead occupy the centers of subclusters in non-virialized clusters (Geller & Beers 1983; Bird 1994; Beers *et al.* 1995).

(d) The fraction of early-type galaxies in our poor groups varies significantly, ranging from that characteristic of the field ($\lesssim 25\%$) to that of rich clusters ($\sim 55\%$). The high early type fractions are particularly surprising, because all of the groups in this sample have substantially lower velocity dispersions (a factor of $\sim$ 2-5) and galaxy number densities (a factor of $\sim$ 5-20) than are typical of rich clusters. Hence, the effects of disruptive mechanisms like galaxy harassment (Moore *et al.* 1996) on the morphology of poor group galaxies are weaker than in cluster environments. In contrast, the kinematics of poor groups make them preferred sites for galaxy-galaxy mergers (Barnes 1985; Aarseth & Fall 1980; Merritt 1985), which may alter the morphologies and star formation histories of some group members. If galaxy-galaxy interactions are not responsible for the high early type fractions, it is possible that the effects of environment are relatively unimportant at the current epoch and that the similarity of the galaxy populations of rich clusters and some poor groups reflects conditions at the time of galaxy formation.

(e) The fraction of early-type group members that have experienced star formation within the last $\sim$ $2h^{-1}$ Gyr is consistent with that in rich clusters with significant substructure ($\sim$ 15%; Caldwell & Rose 1997). If some of the subclusters in these rich, complex clusters are groups that have recently fallen into the cluster environment, the similarity between the star formation histories of the early types in the subclusters and of those in our sample of field groups indicates that the cluster environment and associated mechanisms like ram pressure stripping (Gunn & Gott 1972) are not required to enhance and/or quench star formation in these particular galaxies. If the

recent star formation is tied to the external environment of the galaxies and not to internal instabilities, it is more likely that galaxy-galaxy encounters have altered the star formation histories of some early type galaxies in groups and in subclusters.

Subject headings: galaxies: clustering — galaxies: distances and redshifts — galaxies: elliptical and lenticular, cD — galaxies: evolution — galaxies: interactions — cosmology: dark matter — cosmology: large-scale structure of Universe

1. Introduction

Most galaxies in the local universe, including our own Galaxy, belong to poor groups of galaxies. Despite the ubiquity of the group environment, we know little about the matter content of groups and the evolution of group galaxies outside of the Local Group. Because poor groups typically contain fewer than five bright ($\lesssim M^*$) galaxies, studies to date have been hampered by small number statistics. Some of the critical, unanswered questions are (1) whether poor groups are in fact bound systems with significant populations of fainter members, (2) why many poor groups, with their high galaxy densities, short crossing times, and favorable environments for galaxy-galaxy mergers, survive long enough to be cataloged, and (3) how galaxies might evolve in an environment where the influences of the intra-group medium and the global potential are weak compared with those in rich clusters. The advent of multi-object spectroscopy now makes it possible to address these questions in unprecedented detail. In this paper, we present the first results from a fiber spectroscopic survey of 12 poor groups of galaxies.

The issue of whether many poor groups, even those identified from redshift surveys, are bound systems instead of chance superpositions of galaxies along the line-of-sight has been a puzzle. The existence of one poor group, our Local Group, is unchallenged. In contrast, Ramella *et al.* (1989) show that $\sim 30\%$ of groups of three or four galaxies in the CfA Redshift Survey (Huchra *et al.* 1995) are probably unbound, geometric projections. One useful approach in finding bound systems is to identify those, like certain Hickson compact groups, with apparently interacting members (Rose 1977; Hickson 1982; de Oliveira & Hickson 1994). Yet these systems are also subject to projection effects (*i.e.,* a pair of interacting galaxies with two interlopers; Mamon 1992) and, because they constitute only a small fraction of cataloged groups, may not be dynamically representative. Another strategy is to search for poor groups with diffuse X-ray emission (Mulchaey *et al.* 1993; Ponman & Bertram 1993; Pildis *et al.* 1995), in which the existence of a common gravitational potential is suggested by the intra-group gas (*e.g.,* Ostriker *et al.* 1995). ROSAT images reveal that at least 25% (22 of 85) of Hickson compact groups (Ponman *et al.* 1996) have such an intra-group medium. However, the potentials of some poor groups may be too shallow for emission from hydrostatic gas to reach detectable levels (Mulchaey *et al.* 1996a). It is even possible that the gas, like the galaxies in some cases, is merely a projection of unbound material in a filament alone the line-of-sight (Hernquist *et al.* 1995). To determine whether a poor group is a bound system and to explore its kinematics in detail, we must spectroscopically identify more members. Furthermore, if fainter populations of galaxies do exist in these groups, then we will have the statistics necessary to quantify the mass associated with the galaxy, X-ray gas, and dark matter components and to better understand how galaxies may evolve in such environments.

If some poor groups are bound systems, then another critical question is why they

exist at all. Poor groups have higher galaxy densities than the field and lower velocity dispersions than cluster cores, making them favorable sites for galaxy-galaxy mergers (Barnes 1985). Galaxies are tidally interacting or merging in many Hickson compact groups (de Oliveira *et al.* 1994; Longo *et al.* 1994; Hunsberger *et al.* 1996; Yun *et al.* 1997). The likelihood of mergers and the short group crossing times ($\lesssim 0.05$ of a Hubble time) suggest that most groups should have already merged into one object. Therefore, either bound groups are collapsing for the first time or only a small fraction of the group mass is tied to the galaxies, lowering the rate of galaxy-galaxy interactions relative to a galaxy-dominated system and allowing the group to survive many crossing times (Governato *et al.* 1991; Bode 1993; Athanassoula 1997). To resolve this issue by measuring the underlying mass distribution of poor groups, we need to improve the statistics of group membership with an extensive spectroscopic survey.

Once we know if a group is real and how much mass is associated with its galaxies, we can investigate the influences of group environment on galaxy evolution. For example, because "cD" galaxies in clusters lie in regions of high local density (Beers & Geller 1983; Zabludoff *et al.* 1990; Beers *et al.* 1995), but not always in the center of the global cluster potential, these galaxies may evolve first in poor group-like environments prior to the final collapse and virialization of the cluster as a whole (Merritt 1985). If so, then "cD"s are likely to form via galaxy-galaxy mergers in the center of a collapsing group, where the conditions for mergers are most favorable (Merritt 1984; Tremaine 1990). Over the lifetime of the group, dynamical friction or radial orbits may bring in more galaxies to merge with the "cD." X-ray-detected poor groups, which almost always contain a giant ($\lesssim M_B{}^* - 1$) elliptical near the peak of the X-ray emission, are ideal laboratories for testing this picture of "cD" formation. If the group environment is the birthplace of "cD"s, then the giant elliptical will be coincident with the centroid of the projected spatial distribution of galaxies and will have little peculiar velocity with respect to the mean of the system. An extensive spectroscopic survey of group members will allow us to test this formation hypothesis directly in the poor group environment.

The factors that might affect the evolution of galaxies in poor groups are different from those present in rich clusters. Some of the proposed cluster-based processes, such as ram pressure stripping (Gunn & Gott 1972) and galaxy harassment (Moore *et al.* 1996), are less effective in group environments, where the number density of bright galaxies and the global velocity dispersion are small compared with clusters. The lower velocity dispersions of poor groups suggest instead that galaxy-galaxy interactions (*e.g.*, close tidal encounters or mergers) are likely to dominate any environmentally-dependent evolution of galaxies in groups. If clusters evolve hierarchically by accreting poor groups of galaxies (subclusters), members of an infalling group have recently experienced the hot, dense cluster environment for the first time. Therefore, galaxies in poor groups in the field are a control sample for understanding the factors that

influence the evolution of their counterparts in subclusters. For example, we can compare the morphologies and recent star formation histories of galaxies in the substructures of complex clusters like Coma (Caldwell & Rose 1997) with those of galaxies in poor field groups. Differences between the samples would argue that cluster environment is important in transforming galaxies at the present epoch. On the other hand, the lack of such differences would suggest, as the simplest explanation, either that star formation and morphology are influenced by mechanisms present in both field groups and subclusters, such as galaxy-galaxy encounters, or that the effects of environment on galaxies are insignificant compared with conditions at the time of galaxy formation.

This paper is organized in four sections that address whether poor groups are bound systems, why some groups have not yet disappeared, and how the group environment may affect galaxy evolution. Section §2 describes the the sample of 12 poor groups, the fiber spectra, and the classification of group members as early or late type. We discuss our results in §3, including the membership and global velocity dispersion of each group, the composite group velocity dispersion profile, the location of the dominant elliptical relative to the kinematic and projected spatial centers of groups, the fraction of early type galaxies in groups, and the fraction of these early types that show evidence for recent or on-going star formation. Section 4 summarizes our conclusions.

2. The Data

2.1. The Group Sample

A poor group is defined as an apparent system of fewer than five bright ($\lesssim M_B{}^*$) galaxies. Poor groups in the literature have been identified optically and fall into several classes that can be distinguished by their X-ray properties and bright galaxy morphologies (Mulchaey *et al.* 1996b). Groups with detectable intra-group gas typically have a giant ($\lesssim M_B{}^* - 1$) elliptical that is the brightest group galaxy (BGG) and that lies near or on the peak of the X-ray emission (Mulchaey *et al.* 1996b). In contrast, groups without extended X-ray emission tend to optically resemble the Local Group, which consists of a few bright late-type galaxies and their satellites. If some non-X-ray-detected, late-type-dominated groups evolve via such mechanisms as galaxy mergers, dynamical friction, gas stripping from galaxies, and/or infalling primordial gas, into groups with an central, giant elliptical and a detectable intra-group medium, then groups in transition may form a third class of objects. We would expect the cores of such systems to have signatures of recent dynamical evolution, including interacting galaxies and X-ray gas that does not coincide with the galaxies. Existing

group catalogs, such as the Hickson survey of poor, compact groups (Hickson 1982), contain all three classes of poor groups (*e.g.,* de Oliveira & Hickson 1994; de Carvalho *et al.* 1994). To construct our sample, we select poor groups from these three classes that have complementary ROSAT Position Sensitive Proportional Counter (PSPC) X-ray images.

The sample consists of 12 nearby ($1500 < cz < 8000$ km s^{-1}), optically-selected groups from the literature (NASA/IPAC Extragalactic Database (NED), Helou *et al.* 1991) for which there are existing, sometimes serendipitous, pointed PSPC observations of the fields in which the groups lie. The integration times of the PSPC images are sufficiently long (> 2000 sec; Mulchaey & Zabludoff 1997 (Paper II)) to allow the detection of all groups with X-ray luminosities of $L_X \gtrsim 10^{40} h^{-2}$ erg s^{-1} within this range of radial velocities. These groups are chosen to be accessible from Las Campanas Observatory and to have at least three bright galaxies with known redshifts and magnitudes.

Of the 12 groups, we observed five in August 1995 and seven in April 1996 with the multi-fiber spectrograph (Shectman *et al.* 1992) and 2D-Frutti detector mounted on the du Pont 2.5m telescope at the Las Campanas Observatory. The selection of groups for the first spectroscopic run differed from the second. Before the first run, we did not know which of the five groups had detectable, extended X-ray emission. We chose two groups with the central, giant elliptical characteristic of systems with intra-group media (Mulchaey *et al.* 1996b): NGC 533 and NGC 741. For contrast, we selected three other groups, NGC 491, NGC 664, and NGC 7582, that have optical morphologies more akin to the Local Group. (NGC 664 is a previously uncataloged group, identified as four galaxies at the same redshift in the NED database, whose position on the sky, mean radial velocity, high Galactic latitude, and serendipitous ROSAT pointing made it suitable for the observing program.) Of the seven groups observed during the second run, all were known X-ray detections, including HCG 90, a possible transitional object with several interacting galaxies in its core (Longo *et al.* 1994) and a marginal X-ray detection (Ponman *et al.* 1996). Therefore, our group sample is not representative of published group catalogs, in which less than half of the groups are X-ray-detected. Instead, the sample is weighted toward X-ray groups, because of the likelihood that they are bound systems and the most evolved poor groups.

In the final reduction of the PSPC data, we detect extended emission in nine of the 12 groups: NGC 533, NGC 741, NGC 2563, NGC 4325, NGC 5129, NGC 5846, HCG 42, HCG 62, and HCG 90. The X-ray gas in HCG 90 is asymmetric and not coincident with the galaxies, suggesting that this group is in fact dynamically evolving. The three Local Group-like targets, NGC 664, NGC 491, and NGC 7582, are not detected. Paper II includes a full discussion of the analyses of the X-ray and STScI/Digitized Sky Survey images.

To obtain galaxy targets in each group field over the 1.5×1.5 degree field of the fiber spectrograph, we used coordinates, star/galaxy classifications, and magnitudes from the Automated Photographic Measuring survey (APM, Maddox *et al.* 1990). The uncalibrated, relative magnitudes drawn from the blue plate scans were sufficient to identify the $\sim$ 150 brightest galaxies in each field. Using the STScI/Digitized Sky Survey, we checked all potential targets typed as galaxies by eye, discarding stars and plate flaws. Inspection of the DSS revealed that about $\sim$5-10% of the brightest galaxies were not included in the APM catalog, so we added the most obvious omissions to our final target lists.

To quantify the sample incompleteness due to the underrepresentation of bright galaxies in the APM catalog, we ran the FOCAS program (Jarvis & Tyson 1981) on the STScI/Digitized Sky Survey scan for each group after the completion of both observing runs. We used the FOCAS classification scheme to identify the $\sim$ 150 brightest galaxies in each field. We visually checked all objects typed as galaxies by FOCAS, eliminating stars and plate flaws. Inspection of the scans confirmed that that the FOCAS catalogs were more complete than the APM output, so we adopted the FOCAS catalogs as the master lists from which we subsequently determined the completeness of the group samples (§3.1). We matched the FOCAS coordinates to the APM coordinates and list the former in Table 1.

2.2. The Spectra

We obtain fiber spectra for $\sim$ 50-100 of the brightest galaxies in each of the 12 group fields. In total, we measure 963 galaxy spectra. Each spectrum is extracted from the two-dimensional array, flat-fielded, wavelength-calibrated, and finally sky-subtracted based on the flux normalization of the 5577 Å, 5890 Å, and 6300 Å night sky lines. The spectra have a resolution of $\sim$5-6 Å, a pixel scale of $\sim$ 3 Å, and a wavelength range of 3500-6500 Å. The average signal-to-noise S/N in the continuum around the Hβ λ4861, Hγ λ4340, and Hδ λ4102 absorption lines is typically $\sim$ 8 (calculated by determining the ratio of the mean square deviation about the continuum near each absorption line to the mean continuum at the absorption line, after excluding the absorption line and any nearby sky lines). The 3.5 arcsec fiber aperture subtends projected physical diameters between $0.3h^{-1}$ kpc and $1.2h^{-1}$ kpc at the distances of the groups (from 16 to $72h^{-1}$ Mpc; $q_0 = 0.5$ and $H_0 = 100h$ km s^{-1} Mpc^{-1} are used throughout this paper). Hence, the fibers only sample light from the core of each group member.

We determine the radial velocities using the cross-correlation routine XCSAO and the emission line finding routine EMSAO in the RVSAO package in IRAF (Mink & Wyatt 1995). The velocities in Table 1 are either emission line velocities, absorption line velocities, or a weighted average of the two (see Shectman *et al.* 1997 (their §2.2)

or Lin 1995 for a discussion of the cross-correlation templates and the spectral lines typically observed). We compute velocity corrections to the heliocentric reference frame with the IRAF/HELIO program. By adding 39 galaxy velocities from NED, we obtain a total of 1002 velocities in the group fields. For galaxies projected within $0.3h^{-1}$ Mpc of the group center and brighter than an absolute magnitude of $M_B \sim -17 + 5\log_{10}\ h$, the samples range in completeness from ~ 60 to 100% of the FOCAS catalog (Figure 4), although we observe galaxies out to projected radii as large as $0.95h^{-1}$ Mpc and to limits as faint as $M_B \sim -14$ to $-16 + 5\log_{10}\ h$, depending on the distance to the group.

We estimate the velocity zero-point correction and external velocity error by comparing our velocities with HI velocities from NED. Figure 1 shows the residual for 39 galaxies as a function of our internal velocity error estimate. We use only those HI velocities with quoted errors of < 30 km s^{-1}. The mean residual of 13 km s^{-1} (solid line) is small compared with the *rms* deviation of the residuals (~ 80 km s^{-1}) and is consistent with the mean velocity of 94 stars (-17 km s^{-1}) that were serendipitously observed with the same instrument (dashed line). Therefore, we do not apply a zero-point correction to the velocities.

We adopt the *rms* deviation of the residuals (80 km s^{-1}), which is constant over the range of internal errors, as the true velocity error when the internal or NED error is smaller than 80 km s^{-1}; otherwise, we list the internal or NED error. Our error estimates are consistent with the average external error estimate of $\sim$70 km s^{-1} for the Las Campanas Redshift Survey (Shectman *et al.* 1996), which employs the same fiber spectrograph setup.

2.3. Galaxy Classification

We morphologically classify the group members (as defined in §3.1) that have apparent magnitudes of $m_B \sim 17$ or brighter. This apparent magnitude limit is equivalent to absolute magnitude limits ranging from $M_B \sim -14$ to $-17 + 5\log_{10}\ h$, depending on the distance to the group. The galaxies are typed as either early (E and S0) or late (all others) from R-band CCD images or from STScI/Digitized Sky Survey POSS E or SERC B_J images. The CCD and the scanned plate data overlap for 60% of the 188 typed galaxies, and our classifications from these two media agree. Because we use only two broad classifications, there is complete agreement between the independent classifications of the authors. Our classifications are also ~ 85% consistent with classifications in NED for the 100 group galaxies with published morphologies. Most of the discrepancies arise when our classification is S0/a and NED's type is S0, because we define S0/a transitional galaxies as late types.

Table 1 lists the galaxy name from our catalog, J2000 coordinates from FOCAS using the DSS/STScI plate solution, heliocentric radial velocity (v), type of velocity

measurement (from absorption lines "0", emission lines "1", or a combination of both "2"), morphological classification (either early "e" or late "s" type), and the medium (plate "p" or CCD "c") that we use to classify the galaxy. We note the 39 heliocentric velocities obtained from NED and the references therein with an "N" in the last column. An example of the format of Table 1 is given in the text. The full version of the table that includes the 1002 galaxy velocities in the sample is available on the CDROM accompanying this volume.

3. Results and Discussion

3.1. Group Membership

Are poor groups bound systems or chance superpositions of galaxies along the line-of-sight? Our spectroscopic survey samples the fields of groups whose membership previously totaled less than five bright ($\lesssim M_B{}^*$) galaxies. The detection of a significant population of fainter members would be a first step in demonstrating that these poor groups are not just geometric projections of unbound galaxies.

We determine the galaxy membership of each group from a pessimistic, 3σ-sampling algorithm (Yahil & Vidal 1977). We use the statistical bi-weight estimators of location (mean velocity) and scale (velocity dispersion) to identify 3σ outliers in the distribution of galaxy velocities within ± 3000 km s^{-1} of the center of the main peak (see Beers *et al.* 1990 for a description of the bi-weight estimators). On each successive iteration, the 3σ outliers are removed and the location and scale of the peak re-calculated. We halt the procedure prior to the removal of the last set of outliers.

The resulting membership of each of the 12 groups is indicated by the shaded histograms in Figure 2, which shows the galaxy velocity distributions from 0 to 30000 km s^{-1}. The width of the velocity bins is 250 km s^{-1}, roughly $3\times$ the typical external error. In total, there are 280 group members. The first nine groups are detected by the ROSAT PSPC, the last three are not (see Paper II). The histograms of the X-ray groups reveal large populations of group members down to absolute magnitudes of $M_B \sim -14$ to $-16 + 5\log_{10} h$. Because the membership algorithm can not be applied to the small number of galaxies in the peak of each non-X-ray group, we accept all the galaxies within contiguous bins as group members. As a result, the membership for the non-X-ray groups may be overestimated.

We show the projected spatial distributions of the group members in Figure 3. The angular size of each plot is 1.62×1.62 degrees (the fiber spectrograph field is 1.5×1.5 degrees). Each tickmark corresponds to 5.7 arcmin. Digitized scans of Palomar Sky Survey or UK Schmidt plates from the STScI/DSS are not complete for every group. Hence, we mark the boundary of the unsampled regions with a dashed line: the

westernmost fifth of the NGC 741 field, in the northernmost fifth of the NGC 5129 field, in the northernmost fifth of the HCG 90 field, and the northernmost tenth of the NGC 7582 field. The morphological types of galaxies with apparent magnitudes of $m_B \sim 17$ or brighter are indicated by "0" for early and "S" for late. The filled circles mark the untyped group members. The scale bar below each group name is $0.3h^{-1}$ Mpc. In the X-ray groups, as in rich clusters, the early types concentrate more in the group centers than do the late types. There are no early types in the three non-X-ray groups (see §3.5).

The number counts of group members in the velocity histograms in Figure 2 are not directly comparable, because each group field is sampled over a different physical radius and to a different absolute magnitude. To compare the galaxy number densities of the groups, we subsample each system within a projected radius of $0.3h^{-1}$ Mpc and to an absolute magnitude of $M_B \sim -17 + 5\log_{10}\ h$. Figure 4 shows the observed number counts of group members within these limits (shaded). To roughly compensate for incomplete sampling down to the magnitude limit (completeness is indicated by the fraction above each histogram bar), we assume that the fraction of all unobserved galaxies that are group members is the same as the fraction of all observed galaxies that are members. The white histogram shows these "corrected" group galaxy counts. Our rough calibration of the FOCAS magnitudes introduces more uncertainty into the "corrected" galaxy counts, so a small difference between the counts of two groups is not significant. Also note that the "corrected" counts are lower limits for two groups, NGC 7582 and NGC 5846, for which the 1.5×1.5 degree fiber field corresponds to less than $0.3h^{-1}$ Mpc (0.21 and $0.24h^{-1}$Mpc, respectively). Nevertheless, as this plot shows, non-X-ray-detected groups have lower galaxy densities than are typical of X-ray groups. For the same radial and magnitude cuts, the core of the Coma cluster (NED) has 83 galaxies (a lower limit because we make no correction for incompleteness). Thus, the galaxy density of the Coma core is ∼5-20× that of the poor group cores.

By sampling to deeper magnitudes and to larger radii than past studies, we find that the physical extents of the poor groups in Figure 3, even those of HCG 42, HCG 62, and HCG 90, are larger than the typical values in the literature for Hickson compact groups (Hickson *et al.* 1992). The number densities of galaxies within $0.3h^{-1}$ Mpc and with $M_B \lesssim -17 + 5\log_{10}\ h$ in HCG 42, HCG 62, and HCG 90 (Figure 4) are a factor of $\sim$ 70-700 times lower than those inferred from the brightest four members (Hickson, Kindl, & Huchra 1988). These discrepancies result from the method of selecting Hickson groups, which are defined as concentrations of four or five bright galaxies within a projected radius of $\lesssim 0.1h^{-1}$ Mpc (see also de Carvalho *et al.* 1994). The galaxy number densities of the Hickson compact groups are not significantly different from those of the other poor groups in our sample. In general, the presence or absence of diffuse X-ray emission better differentiates between poor groups of high and low galaxy densities (and velocity dispersions (§3.2) and early type fractions (§3.5)).

Could the X-ray groups be superpositions of three or four unbound, field galaxies and their fainter satellites? This explanation is unlikely, because the central, giant elliptical is not typical of field galaxies and the early type galaxies tend to concentrate in the group core. In addition, studies of the satellite populations of $\lesssim M_B{}^*$ field galaxies with the same fiber spectrograph setup (Zaritsky *et al.* 1997), within similar projected radii from the primary galaxy, and to comparable absolute magnitude limits as our group sample find on average one satellite for each primary. The ratios of faint to giant galaxies in the X-ray groups exceed that expected from satellite statistics alone.

The large populations of fainter galaxies and the central concentration of early types in the X-ray groups suggest that these groups are bound systems. The dynamical state of the non-X-ray groups is less obvious. In §3.2, 3.3, and 3.4, we use the global kinematic properties, the velocity dispersion profile, and the position of the central, giant elliptical relative to the kinematic and projected spatial group centroids as additional tests of whether the X-ray groups are bound and possibly virialized.

3.2. Group Velocity Dispersions

3.2.1. Results

To date, the line-of-sight velocity dispersions (σ_r) of poor groups have been uncertain due to their determination from only a few galaxies. This uncertainty has translated into a large uncertainty in cosmologically important properties like the underlying mass distribution and the global baryon fraction. Because we increase the membership by a factor of 10 in many of our groups, we can, for the first time, determine poor group l-o-s velocity dispersions with sufficient precision ($\lesssim 20\%$) that the differences among them are statistically meaningful. The calculation of the mean velocity $\overline{v}$ and σ_r for each group is based on the bi-weight estimators of location and scale (Beers *et al.* 1990) corrected for cosmological effects. These estimators are more robust than the standard mean and velocity dispersion (*e.g.*, Danese *et al.* 1980), but, for this sample, the standard velocity dispersion is always within the 68% confidence limits of σ_r. The velocity dispersions of the X-ray groups range over more than a factor of two, from 190 km s^{-1} in HCG 90 and 210 km s^{-1} in HCG 42 to 430 km s^{-1} in NGC 741 and 460 km s^{-1} in NGC 533.

The results of §3.3 argue that the group velocity dispersion remains fairly constant with radius out to at least $0.5h^{-1}$ Mpc. However, to confirm that the range of velocity dispersions above does not result from the different physical radius to which each group is sampled by the fixed angular size of spectrograph field, we determine the membership and the velocity dispersions within a $0.3h^{-1}$ Mpc radius. The resulting

σ_r's are indistinguishable within the 68% confidence errors from those determined from all the data. Therefore, we use the $\overline{v}$ and σ_r determination from all the group members in subsequent analyses.

Table 2 lists the group, the group optical projected centroid in J2000 (unweighted by luminosity), the total number of galaxies with measured redshifts in the fiber field N_{tot}, the number of group members N_{grp}, the bi-weight estimators of the mean heliocentric velocity $\overline{v}$ and the line-of-sight velocity dispersion σ_r, and the physical radius of the group sampled by the fiber field r_{samp}. For the groups where $r_{samp} \geq 0.67$ (the median pairwise radius r_p for CfA Redshift Survey groups (Ramella *et al.* 1989)), we tabulate r_p, the mean harmonic (virial) radius r_h, the virial mass M_{vir}, and the ratio of the crossing time to a Hubble time t_c/t_H. These last four kinematic quantities are calculated as in Ramella *et al.* (1989). For the five groups with calculated masses and crossing times, r_{samp} is $\gtrsim 20\%$ larger than r_p, suggesting that the limited size of the fiber field does not artificially reduce our estimate of the group extent and bias the kinematic determinations.

The median value of the harmonic radius of the four X-ray groups is $0.41h^{-1}$ Mpc, consistent with the median $r_h = 0.5h^{-1}$ Mpc for groups in the CfA Redshift Survey (Ramella *et al.* 1989). However, r_h depends on how the distribution of galaxies is biased with respect to that of the dark matter in the system. To check that the harmonic radius is an accurate estimate of the virial radius, we calculate the radius r_{500} that corresponds to an overdensity of 500, where N-body simulations show that the dynamical equilibrium hypothesis is satisfied (Evrard, Metzler, & Navarro 1996). For a poor group with an X-ray temperature typical of our X-ray groups (about 1 keV, Paper II), $r_{500} = 1.24\sqrt{(kT/10 \text{ keV})}\ h^{-1}$ Mpc $= 0.4\ h^{-1}$ Mpc. Therefore, we conclude that biasing between the galaxies and dark matter does not significantly affect the estimates of the kinematic quantities in Table 2.

The velocity dispersions of poor groups in the literature are usually estimated from the four or five brightest members. With our deeper redshift samples, we can determine the accuracy of these past estimates. The velocity dispersions calculated from only the five brightest galaxies in each group σ_5 tend to underestimate σ_r, because the tails of the galaxy velocity distribution are not well-sampled. In the worst case in our sample, the NGC 2563 group, σ_5 underestimates σ_r by a factor of three. In total, σ_5 underestimates σ_r by more than a factor of 1.5 for five of the nine X-ray groups. The difference between σ_5 and σ_r for the non-X-ray groups is small, because we calculate σ_r itself from only ~ 5 galaxies.

3.2.2. Implications

The $\sim$ 20-50 group members, the central concentration of early type galaxies, and the short crossing times ($\lesssim 0.05$ of a Hubble time) of the X-ray groups suggest that

they are bound systems, not geometric superpositions of galaxies, and that the group cores are close to virialization or virialized. Because we do not detect diffuse X-ray emission or a significant fainter population in the three non-X-ray groups, we are unable to determine their dynamical state. The non-X-ray groups, which consist of one or two L^* or brighter spirals with several fainter galaxies that may be satellites, are morphologically akin to the Local Group (although our samples are not sufficiently deep to ascertain whether any group has a dwarf spheroidal population like that of the Local Group; van den Bergh 1992). If the non-X-ray groups are dynamically similar to the Local Group, they are bound (see Zaritsky 1994). Our current data do not exclude this possibility — the velocity dispersions of the non-X-ray groups are consistent with the upper limits on their X-ray luminosities (Paper II). If the non-X-ray groups are bound, but are collapsing for the first time like the Local Group (cf. Zaritsky 1994), the virial mass of systems like NGC 664 in Table 2 is uncertain by a factor of two (as the system is not yet virialized). If the non-X-ray groups are just chance superpositions, their kinematic quantities in Table 2 do not represent the properties of bound groups.

3.3. Velocity Dispersion Profile

3.3.1. Results

The ratio of the mass associated with group galaxies to the mass associated with the common group halo determines the timescale of galaxy-galaxy interactions and thus the group's ability to survive for more than a few crossing times (Governato *et al.* 1991; Bode 1993; Athanassoula 1997). The statistics of our sample make analyzing group kinematics on an individual basis difficult. To obtain an understanding of the underlying mass distribution in poor groups, we combine the velocity and projected spatial distributions of all of the X-ray group members.

Figure 5 shows the velocity offset vs. the projected radial offset of 204 X-ray group members from the central, giant elliptical (the brightest group galaxy, hereafter BGG). The velocity difference is normalized with the internal velocity dispersion of the BGG (σ_{BGG}). We include only the seven X-ray groups for which σ_{BGG} is known (HCG 42, HCG 90, NGC 2563, NGC 5129, NGC 5846, NGC 533, NGC 741; McElroy 1995; Trager 1997). We calculate the normalized velocity dispersion δ (i.e., the *rms* deviation in the normalized velocity offset) within each radial bin (dashed lines).

The velocity dispersion of the combined group sample does not decrease significantly with radius from the central $\sim 0.1h^{-1}$ Mpc to at least $\sim 0.5h^{-1}$ Mpc, in contrast to the more than factor of two decrease in δ that would be observed if the entire mass were concentrated within the first bin. The extended mass is either in the galaxies, in a common halo through which the galaxies move, or in both the galaxies and a diffuse

halo. If all the mass were tied to the galaxies, most of the mass would be associated with the bright, central elliptical in those groups in which the BGG dominates the light. For groups with a few galaxies that have luminosities comparable to the BGG, δ would be increased at large radii by subgroups consisting of a massive galaxy and the subgroup members that are orbiting it. If this picture were accurate, we would expect the δ profiles of groups with several comparably bright galaxies to be shallower than those in which the BGG is dominant. However, the combined velocity dispersion profile of a subsample of two groups (HCG 42 and NGC 741) in which the BGG dominates the light (*i.e.*, the BGG luminosity exceeds the combined luminosity of the other L^* or brighter galaxies) is indistinguishable from that of the entire sample. Therefore, we conclude that most of the group mass lies in a smooth, extended dark halo.

Is this halo associated with the group as a whole or with the BGG? If a galaxy forms inside a dark halo through dissipative collapse (cf. Blumenthal *et al.* 1986), baryons concentrate in the center, deepening the gravitational well and increasing the velocity dispersion of the galaxy relative to that of the halo. In all the radial bins in Figure 5, $\delta > 1$, indicating that the BGG is on average dynamically *cooler* than the surrounding group. Thus, it is likely that the dark halo belongs to the group and not to the central, giant elliptical (note that the group velocity dispersion profile does not decrease with radius when the velocity and projected radial offsets are defined relative to the group mean velocity and projected spatial centroid, as in Figure 6a). We reach the same conclusion in Paper II by examining the X-ray images and spectra of the hot gas in these groups.

It is possible that contamination from galaxies not bound to the group artifically increases the velocity dispersion of the combined group sample, especially at large radii from the BGG. We can conservatively estimate the degree of contamination by defining the 12 galaxies in the fifth (last) bin in Figure 5 with peculiar velocities $> 1.33\sigma_{BGG}$ and $< -1.33\sigma_{BGG}$ as interlopers. Because the interloper fraction should be constant with peculiar velocity, we predict that there are a total of about $12(3/2) = 18$ interlopers in the fifth bin. The ratio of the areas sampled by the fourth and fifth bins is 0.24. Therefore, only about four of the galaxies in the fourth bin and one or none of the galaxies in each the inner three bins are likely to be interlopers. Even excluding the four galaxies with the most extreme peculiar motions from the fourth bin only decreases the velocity dispersion in this bin by 15% to $\delta = 1.1$. We conclude that the shape of the combined velocity dispersion profile within $0.5h^{-1}$ Mpc is not significantly affected by outliers.

3.3.2. The Mass of Group Halos

The virial masses of the poor X-ray groups are $M_{vir} \sim 0.5\text{-}1 \times 10^{14} h^{-1} M_\odot$. What fraction of this mass is in the common group halo and what fraction is associated with

group galaxies? We expect that early in a group's evolution, the individual galaxy halos are tidally-limited by the global potential of the group (cf. Peebles 1970; Gunn 1977). We must first estimate the tidal extent of the halos of X-ray group members before we can estimate their masses. Using Merritt's (1984) approach, we assume that the group's potential is in the form of an analytic King model (King 1972)[†]. The maximum tidal radius of a galaxy near the core of a group is $r_T \approx \frac{1}{2}(r_c\sigma_g/\sigma_r)$, where we adopt $r_c \sim 125h^{-1}$ kpc as the group's core radius (equivalent to the cluster value; Bahcall 1975) and σ_g as the galaxy's internal, line-of-sight velocity dispersion. For L^* galaxies ($\sigma_g \approx 225$ km s^{-1}; Tonry & Davis 1981) in groups with velocity dispersions of $\sigma_r = 200$ and 450 km s^{-1}, the maximum tidal radii are ~ 75 and $35h^{-1}$ kpc, respectively, which are larger than the luminous radii typical of such galaxies. These values of r_T are less than the $> 150h^{-1}$ kpc dark halos of isolated disk galaxies (Zaritsky & White 1994), but greater than the predicted, tidally-limited extent of galaxies in the cores of rich clusters ($\sim 15h^{-1}$ kpc, Merritt 1984).

What is the fraction of the group mass associated with its galaxies? We estimate the tidally-limited mass of an L^* galaxy from the virial theorem: $m \approx \frac{1}{2}(r_T\sigma_g^2/G)$ for a King model (1966). For L^* galaxies in a $\sigma_r = 200$ and 450 km s^{-1} group, we obtain $m^* \sim 4 \times 10^{11}$ and $2 \times 10^{11}h^{-1}$ $M_\odot$, respectively. To estimate the mass of the brighter, central elliptical, we assume that its internal velocity dispersion is $\sigma_{BGG} \sim 300$ km s^{-1} (typical of the central, giant elliptical in our X-ray groups) and that its radius is $\sim 100h^{-1}$ kpc (which is between r_T and r_c, a range consistent with the effective optical radii of "cD" galaxy envelopes (Schombert 1988), with the maximum radius to which the X-ray emitting gas in a BGG is detected (Paper II), and with the possibility that the BGG is less tidally-limited than other group members, because of its position in the group center (§3.4) where the tidal forces are symmetric and relatively weak (Merritt 1984)). We obtain $\sim 10^{12}h^{-1}$ $M_\odot$ as an estimate of the mass of the BGG's in the sample groups. For a group like NGC 741, the mass associated with the four L^* or brighter galaxies within the virial radius $r_h = 400h^{-1}$ kpc is then $\sim 10^{12} + 3(2 \times 10^{11})h^{-1}$ $M_\odot \approx 2 \times 10^{12}h^{-1}$ $M_\odot$.

We can also estimate the fraction of mass tied to fainter group galaxies. Assuming that the luminosity spectrum of group galaxies is a Schechter function (1976) with $\gamma = 1.25$ and a lower cut-off at $0.05L^*$ ($L^* \sim 1 \times 10^{10}$ $L_\odot$; Kirshner *et al.* 1983), we use the empirical luminosity-velocity dispersion relationship ($L \propto \sigma_g^4$; Faber & Jackson 1976), the equation for tidal radius ($r_T \propto \sigma_g$), and the virial theorem ($m \propto \sigma_g^2 r_T$) to convert the luminosity function into a tidally-limited mass function (see Merritt 1984

[†]Although cosmological simulations predict a somewhat different form for the density profile (Navarro *et al.* 1996), we use a King profile because (1) it is a good fit to the data (cf. Paper II) and (2) we wish to be consistent with past analyses of rich clusters.

for a similar discussion). We obtain

$$dn = \frac{4}{3} e^{-\left(\frac{m}{m^*}\right)^{4/3}} \left(\frac{m}{m^*}\right)^{(1-4\gamma)/3} d\left(\frac{m}{m^*}\right)$$

for galaxies with tidally-limited masses greater than $0.1m^*$, where we assume that the halos of all galaxies are tidally-limited during a close passage to the group core and that only non-luminous matter is removed. The mass of the L^* or brighter members is $\sim 20\%$ of the total galaxy mass. Therefore, the total mass in galaxies in NGC 741 is $\sim 1 \times 10^{13} h^{-1}\ M_\odot$, in contrast to the the virial mass of $\sim 1 \times 10^{14} h^{-1}\ M_\odot$. The fraction of mass in the galaxies within the virial radius is then roughly 10%. In lower velocity dispersion groups such as NGC 4325, there are fewer bright members, but the galaxy halos are less tidally-limited and the virial mass is smaller. Hence, galaxies comprise a greater fraction of the total mass within the virial radius, $\sim 20\%$.

The dominant source of uncertainty in the estimation of the fraction of group mass associated with individual galaxies is the galaxy halo mass. The degree to which group galaxy halos are tidally-limited depends on such key unknowns as the details of galaxy halo formation, the initial orbits of the group members, and the evolution of the group's mass density. It is also possible that additional mass could be collisionally-stripped from galaxies later in the evolution of the group (see §3.5). The exploration of these effects awaits improved simulations.

3.3.3. Implications

The small fraction of the group mass associated with its galaxies will increase the timescale for galaxy-galaxy interactions, such as mergers, close tidal encounters, and dynamical friction, by decreasing the cross-sections of the galaxies (Governato *et al.* 1991; Bode 1993; Athanassoula 1997). This result argues that poor groups survive longer than predicted by models in which all the mass is tied to individual galaxies and may explain why so many poor groups are observed in lieu of single merger remnants.

3.4. The Giant Elliptical vs. the Group Centroid

3.4.1. Results

The poor groups with diffuse X-ray emission in our sample have a giant ($\lesssim M_B{}^* - 1$) elliptical that lies within $\sim$ 5-10h^{-1} kpc of the X-ray peak (Paper II). The coincidence of the BGG position and the X-ray peak suggests that BGG's lie in the center of the group potential. However, it is possible that X-ray emission in the core is dominated

by light from the BGG, hiding an offset between the galaxy and the center of the potential as defined by peak of the intra-group medium. Therefore, the optical data are required to determine whether the BGG is at rest with respect to the group as a whole. In this section, we test this hypothesis in two ways, asking (1) whether BGG's are more concentrated in the core than other group members and (2) whether the radial velocity and projected position of the BGG's are consistent with the kinematic and projected spatial centroids of the groups.

How are the BGG's distributed in projected radius and peculiar velocity compared with other group galaxies? Figure 6a shows the kinematic (y) and projected spatial (x) offsets of the BGG (filled squares) and other group members (filled circles) from the group centroid for the nine X-ray groups. Neither the projected spatial centroid ($\langle r \rangle$) nor the mean velocity ($\langle v \rangle$) of the group are weighted by galaxy luminosity, so the velocity and projected position of the BGG do not bias the centroid calculations. The velocity offset of each galaxy from the mean velocity of the group is divided by the group velocity dispersion σ_r to compensate for differences in the size of the group global potentials.

We define a statistic $R^2 = (x/\delta_x)^2 + (|y|/\delta_{|y|})^2$, where δ_x and $\delta_{|y|}$ are the rms deviations in x and $|y|$ for the entire sample. Thus, a galaxy that has a large peculiar motion and/or that lies outside the projected group core will have a larger R value than a galaxy at rest in the center of the group potential. Figure 6b shows the distributions of R for all of the group members (solid) and for the subset of BGGs (shaded). A Student's t-test gives $< 3 \times 10^{-5}$ as the probability that the means of the non-BGG and BGG distributions are consistent. Therefore, the BGG's are significantly more concentrated in the core, suggesting that BGG's occupy the center of the potential on orbits different from those of other group members.

Are the peculiar velocities and projected positions of the BGG's consistent with the kinematic and projected spatial centers of the groups? The y errorbars in Figure 6a represent the 68% confidence limits on y (ϵ_y) obtained from adding the errors in the group mean velocity and the BGG velocity in quadrature. To estimate the 68% error in x for a BGG in a group with N_{grp} members, we use a statistical jackknife test in which samples of N_{grp} galaxies are drawn from HCG 62, the group with the most members. For each BGG, we adopt the rms deviation in the distribution of x (ϵ_x) for these samples as the x error. (For the BGG in HCG 62, we use the smallest x error calculated among the other groups). The heavy line in Figure 6b shows the distribution of R obtained by assuming that all of the BGG's lie in the centers of their groups. For each BGG, we model the distributions of errors about the center in $|y|$ and in x as Gaussian with rms deviations equal to $\epsilon_y/\delta_{|y|}$ and ϵ_x/δ_x, respectively. The heavy line is the distribution in R that results from 1000 random draws from the model distributions of x and $|y|$ for each BGG. A t-test fails to differentiate between the means of the model R distribution and that of the BGGs (shaded) at better than

the 95% confidence level. We conclude that, to within the errors, the BGG's occupy the center of the group potential.

3.4.2. Timescales for BGG Evolution

The presence of a giant elliptical at rest in the center of each X-ray group is consistent with the picture in which BGG's form from galaxy mergers early in the group's evolution (Merritt 1985; Bode 1994). BGG formation may occur during the initial collapse of the group, before galaxy halos are tidally-truncated and merger rates decline (Merritt 1985). The absolute magnitudes of the BGG's place them in the class of bright ellipticals whose morphologies and kinematics are consistent with merger evolution ($M_B \lesssim -20 + 5\log_{10}\ h$; Kormendy & Bender 1996; Merritt & Tremblay 1996). Such a galaxy may be forming in HCG 90. The total luminosity of the several merging galaxies in HCG 90's core is comparable to the absolute magnitudes of the BGG's in the other X-ray groups.

Do BGG's continue to experience mergers after their formation? The BGG's in our sample show no signatures of later mergers with massive galaxies; their spectra do not indicate recent star formation, their morphologies are not obviously disturbed, and their position in the center of the X-ray emission argues against recent disruptions of the surrounding gas by mergers. For example, one BGG (NGC 5846) is classified as an intermediate age elliptical (the last star formation event occurred more than $\sim$ 6-7h^{-1} Gyr ago; Trager 1997). However, NGC 2300, the central, giant elliptical in the first poor X-ray group discovered (Mulchaey *et al.* 1993), has shells (Schweizer & Seitzer 1992; Forbes & Thomson 1992) and a spectrum that includes a young stellar population ($\lesssim 2h^{-1}$ Gyr old; Trager 1997). Thus, there is some indirect evidence that at least one BGG has experienced a late merger.

We can estimate whether the central elliptical is likely to grow via subsequent mergers with other group members. One possible mechanism is the accumulation of slow-moving, massive galaxies in the group core by dynamical friction. To determine the effects of dynamical friction, we roughly estimate the largest radius from which an L^* galaxy could fall into the center of a group in a Hubble time. We use the dynamical friction timescale (Binney & Tremaine 1987; their eq. 7-26) and the Coulomb logarithm definition (7-13b) for an L^* galaxy on an initially circular orbit to solve for the maximum radius. We use the tidally-limited masses of an L^* galaxy in a σ_r = 450 km s^{-1} and 200 km s^{-1} group from §3.3. For a galaxy moving with circular velocity $v_c = \sqrt{2}\sigma_r$, the maximum radius ranges from $\sim 250h^{-1}$ kpc for the high velocity dispersion group to $400h^{-1}$ kpc for the low σ_r group. This timescale estimate is consistent with simulations (Merritt 1984), which predict that dynamical friction can cause 1-2L^* worth of merger candidates to accumulate in the core of a

$\sigma_r = 500$ km s^{-1} group within a Hubble time. If these candidates do merge with the BGG, some enhancement of the BGG's luminosity is possible, and the luminosity segregation resulting from dynamical friction might then be hidden by the mergers. In contrast, the same equations and simulations predict that an L^* galaxy in a rich cluster ($\sigma_r \sim 1000$ km s^{-1}) requires an improbable $\sim 40h^{-1}$ Gyr to fall to the center from an initial radius of $250h^{-1}$ kpc.

3.4.3. Implications

The existence of a central, giant elliptical in the X-ray groups has implications for the formation of "cD" cluster galaxies (Matthews, Morgan, & Schmidt 1965). The method by which "cD"s evolve is unknown, but there is indirect evidence that these galaxies form outside the cores of rich clusters. For example, "cD"s are not always at rest with respect to the cluster potential, but lie instead in local overdensities (Beers & Geller 1983; Beers *et al.* 1995). In addition, the presence of a "cD" does not depend on the global kinematic properties of the cluster (*i.e.,* clusters that contain a "cD" have similar velocity dispersions to those that do not, Zabludoff *et al.* 1990). Our observations suggest that "cD"s form from galaxy-galaxy mergers in poor groups. Because poor group velocity dispersions are comparable to the internal velocity dispersions of their galaxies, the probability that a galaxy-galaxy collision will lead to a merger is higher in groups than in clusters (see §3.5). Poor groups with central, massive ellipticals may later merge to form clusters or fall into existing clusters (Merritt 1985; Beers *et al.* 1995). In this picture, the BGG would be displaced for a time from the center of the cluster potential. We note that the NGC 2563 X-ray group is one of the groups in Cancer (Bothun *et al.* 1983), an association of groups likely to evolve into a rich cluster after its virialization. In future work, we will use deep optical surface photometry to determine whether the BGG's in the X-ray groups have the extended halos of "cD" galaxies in rich clusters.

3.5. Group Early-Type Fractions

3.5.1. Results

The effects of environment on galaxy evolution are poorly understood. The study of poor groups provides a critical link between the evolution of isolated galaxies in the field and of galaxies subject to the hot, dense environments of clusters. Despite the usefulness of group galaxies as a control sample, their properties, especially at faint magnitudes, are not well-known. One possible test of environmental influences is to

compare the morphologies of group members with those of field and cluster galaxies. Previous work suggests that the fraction of early type (E and S0) galaxies in X-ray detected groups varies widely and that some X-ray groups have no late types among their brightest members (Ebeling *et al.* 1994; Pildis *et al.* 1995; Henry *et al.* 1995; Mulchaey *et al.* 1996b). However, these studies typically include only the four or five brightest galaxies, which biases samples toward ellipticals, and target only the central $\lesssim 0.3h^{-1}$ Mpc, where early types concentrate (*e.g.*, Figure 3). Therefore, to compare the morphologies of group and cluster members, we must sample both environments to similar physical radii and absolute magnitude limits.

We plot the distribution of the early type (E, S0) fractions f of the 12 sample groups in Figure 7. In the X-ray groups, f ranges widely from $\sim 55\%$ (HCG 62, NGC 741, and NGC 533) to $\sim 25\%$ (*e.g.*, NGC 2563). The lower value of f for the X-ray groups is characteristic of the field ($\sim 30\%$; Oemler 1992). We find no early types among the 6-8 galaxies in each of the three non-X-ray groups (shaded).

We can test whether the groups with the highest early type fractions, such as NGC 533 (14 of 25) and NGC 741 (10 of 18), are statistically different from the field. The likelihood of at least k successes in n Bernoulli trials with success probability f_F is $\sum_j \frac{n!}{j!(n-j)!} {f_F}^j (1-f_F)^{n-j}$ for all j such that $n \geq j \geq k$. The fraction of field galaxies that are E's and S0's (f_F) is $\sim 30\%$ (Oemler 1992). If we assume that the E and S0 fraction in NGC 533 is actually consistent with f_F, the probability of finding 14 or more early types in a sample of 25 group members is very small, 6×10^{-3}. The probability that the early type fraction in NGC 741 is consistent with the field is also small, 2×10^{-2}. When these probabilities are considered together, the hypothesis that the early type fractions of both groups are consistent with the field is rejected at the $\sim 4\sigma$ level. NGC 533, NGC 741, and HCG 62 are sampled to physical radii and absolute magnitude limits similar to NGC 2563, an X-ray group in which f is consistent with the field, and to NGC 644, a non-X-ray group in which f is much lower than the field (0%). We conclude that the spread in the distribution of f in Figure 7 is statistically significant.

How do the early type fractions of $\sim 55\%$ in NGC 533, NGC 741, and HCG 62 (16 of 30) compare with values typical of rich clusters? These three groups are sampled to physical radii of ~ 0.6-$0.8h^{-1}$ Mpc, and their members are typed to absolute magnitude limits of $M_B \sim -16$ to $-17 + 5\log_{10} h$. Within this range of radii, the early type fractions of rich clusters are ~ 0.55-0.65 (Whitmore *et al.* 1993). Because the absolute magnitude of the Whitmore *et al.* sample ($M_B \sim -18 + 5\log_{10} h$) is brighter than ours, the cluster early type fractions are relatively biased toward ellipticals. Cutting the group data at the brighter M_B limit worsens the statistics, but increases f. For example, six of the seven galaxies in NGC 533 brighter than the Whitmore *et al.* limit are E's or S0's. Likewise, five of the remaining six members of NGC 741 are early types. Therefore, it is conservative to conclude that the early type fractions in

some poor groups are comparable to those in rich clusters.

3.5.2. The Early Type Fraction-Velocity Dispersion Relation

The inset in Figure 7 shows the correlation between early type fraction and group velocity dispersion for the 12 sample groups. The solid line is an unweighted fit to the data, the dashed line is a fit weighted by the velocity dispersion errors. In both cases, the correlation between morphology and velocity dispersion is significant at the > 0.999 level. The relation is surprisingly robust, given that the groups are sampled over a range of physical radii (~ 0.2-$1.0h^{-1}$ Mpc) and absolute magnitude limits ($M_B \sim -14$ to $-17 + 5\log_{10}\ h$). It is possible that the relation is artificially strengthened by the three non-X-ray groups, which may not be bound. We note, however, that the Local Group would similarly anchor the tail of the correlation. The form of the relation cannot be the same for rich clusters — our fit to the group data predicts that the early type fraction in a $\sigma_r \sim 1000$ km s^{-1} cluster is an unphysical $f = 124\%$. Therefore, the relation must turn up between the poor group and rich cluster regimes. The group $f - \sigma_r$ relation implies either that galaxy morphology is set by the local potential size at the time of galaxy formation (Hickson, Huchra, & Kindl 1988) and/or that σ_r and f increase as a group evolves (Diaferio *et al.* 1995).

3.5.3. Galaxy-Galaxy Collision Timescales

If environment does alter the morphologies of group galaxies after the formation of the group, which environmental influences are most important? Proposed mechanisms to disturb the distribution of stars in cluster galaxies include the tidal shocking of stellar disks by the global potential (B. Moore 1997, priv. comm.), galaxy-galaxy harassment (Moore *et al.* 1996), collisional stripping (*e.g.*, Richstone 1975), and mergers (*e.g.*, Barnes 1989; Weil & Hernquist 1996). Strong tidal shocks could strip the stellar disks from Sc or Sd galaxies passing through the strong gravitational field of the group core, producing remnants consistent with the mass profiles of dwarf elliptical galaxies (B. Moore 1997, priv. comm.); however, only four of the 72 galaxies in our early type sample are as faint as dE/dSph's (*i.e.,* $M_B \gtrsim -16 + 5\log_{10}\ h$), so we do not consider this mechanism in interpreting the group data. Galaxy harassment is not likely to operate effectively in groups, where the number density of bright galaxies and the global velocity dispersion are much smaller than in clusters (B. Moore 1997, priv. comm.). In the following discussion, we calculate the likelihood of galaxy-galaxy encounters (collisions, mergers) by adapting simple models applied in the past to rich clusters (cf. Richstone & Malumuth 1983; Merritt 1984).

Galaxy-galaxy interactions are known to significantly affect galaxy morphology (*e.g.*, Schweizer 1986, Hibbard *et al.* 1994). Observations of poor compact groups suggest that close tidal interactions and accretion events play a role in the evolution of some group galaxies. For example, the isophotes of compact group ellipticals are typically more irregular than those of ellipticals in cluster environments (Zepf & Whitmore 1993), and the fraction of group members with disturbed morphologies and peculiar kinematics is larger than for field galaxies (Rubin *et al.* 1991; de Oliveira & Hickson 1994). If poor groups are longer-lived than previously supposed, and merged galaxies have had more time to relax, the fraction of merger remnants in groups may be even higher than indicated by short-lived merger signatures.

What is the timescale for galaxy-galaxy encounters in our poor groups? We now examine the timescales in four cases: (a) an L^* galaxy in a $\sigma_r = 450$ km s^{-1} group, (b) a galaxy of typical luminosity L_{typ} in a $\sigma_r = 450$ km s^{-1} group, (c) an L^* galaxy in a $\sigma_r = 200$ km s^{-1} group, and (d) an L_{typ} galaxy in a $\sigma_r = 200$ km s^{-1} group.

Definition of Collision Timescale. Following Richstone & Malumuth (1983), we define the collision time as $T_{col} = [\overline{n}\pi {r_T}^2\sqrt{2}\sigma_r]^{-1}$, where $\overline{n}$ is the mean number density of galaxies within the half-mass radius, r_T is the tidal radius of the galaxy, and $\sqrt{2}\sigma_r$ is the typical encounter velocity in an isotropic system. We assume that the group mass distribution inside the virial radius is described by a King model (1966) with a core radius of $r_c \sim 125h^{-1}$ kpc and with a shape defined by the ratio of the group tidal radius to r_c, $R_T/r_c = 20.2$ (see Bahcall 1977 and Dressler 1978 for discussions of the shapes and sizes of clusters). The half-mass radius of this model is $2.83r_c = 354h^{-1}$ kpc, comparable to the typical group virial radius. Therefore, we calculate $\overline{n}$ using the mass within the virial radius. The mean mass of a group member for the tidally-limited mass function defined in §3.3 is $\overline{m} = 0.35m^*$, where m^* is the mass of an L^* galaxy.

(a) L^* Galaxy in a $\sigma_r = 450$ km s^{-1} Group. To calculate T_{col} for an L^* galaxy in a $\sigma_r = 450$ km s^{-1} group, we use the NGC 533 group as an example. In §3.3, we found $r_T \sim 35h^{-1}$ kpc for an L^* galaxy in this group. What is $\overline{n}$? The total mass of NGC 533 within $r_h = 400h^{-1}$ kpc is $M_{vir} \sim 1 \times 10^{14}h^{-1}\ M_\odot$. Thus, if we assume that NGC 533 is spherical and that $f_{halo} \sim 90\%$ is the fraction of the total mass not tied to the galaxies, then the average galaxy number density within r_h is $\overline{n} = (3M_{vir}/4\pi {r_h}^3)(1 - f_{halo})/\overline{m} \sim 529h^3$ Mpc^{-3}. This calculation shows that we would overestimate $\overline{n}$ and thus underestimate the collision timescale by a factor of 10 by assuming that all of the group mass is associated with the galaxies. Note also that f_{halo} is assumed to be constant over time, as would be the case if the tidal limitation of the galaxies occurred early in the group's evolution. If f_{halo} increases in time, then the collision timescales below are somewhat overestimated.

With these values of $\overline{n}$ and r_T, we obtain $T_{col} \sim 0.07\times$ a Hubble time — an L^* galaxy experiences a collision in every $\sim$ four crossing times. In comparison, a rich cluster like Coma has at least $\sim 5\times$ the galaxy number density and more than twice

the velocity dispersion of NGC 533. If cluster galaxies have halos truncated to about half the extent of those in NGC 533 (Merritt 1984), then the collision time for an L^* galaxy in a rich cluster is ~ 0.04 of a Hubble time. Therefore, over the same period of time, an L^* galaxy in a rich cluster is nearly twice as likely to experience a collision as an L^* galaxy in NGC 533, the poor group with the shortest estimated T_{col} in the sample.

(b) L_{typ} Galaxy in a $\sigma_r = 450$ km s^{-1} Group. To understand more about how the collision history of a galaxy depends on its luminosity and on the velocity dispersion of the group, we estimate the collision time for a typically bright galaxy in NGC 533. The value of $\overline{n}$ is the same as in case (a), but what is r_T? The luminosity of a typically bright galaxy is $L_{typ} \approx 0.15L^*$ for the Schechter luminosity function assumed in §3.3 (Richstone & Malumuth 1983). L_{typ} is two magnitudes fainter than L^* and is also the approximate limit at which the completeness of our group samples is at least $\sim 60\%$ (§3.1). We use the Faber-Jackson (1976) relation and the internal velocity dispersion of an L^* galaxy (≈ 225 km s^{-1}; Tonry & Davis 1981) to estimate σ_g for an L_{typ} galaxy (~ 140 km s^{-1}). The tidal radius of an L_{typ} galaxy is then $\sim 20h^{-1}$ kpc, and the collision time is about three times longer than for an L^* galaxy in NGC 533.

(c) L^* Galaxy in a $\sigma_r = 200$ km s^{-1} Group. An L^* galaxy in a lower velocity dispersion group will collide less frequently than will its counterpart in NGC 533. The tidal radius of this galaxy is $\sim 75h^{-1}$ kpc (§3.3). What is $\overline{n}$? For a $\sigma_r = 200$ km s^{-1} group, we estimate the virial mass within $400h^{-1}$ kpc by assuming that the virial radii are the same and scaling NGC 533's M_{vir} by the square of the ratio of the velocity dispersions of the two groups. Because (1) the virial mass is smaller, (2) the average galaxy mass is larger, and (3) $f_{halo} \sim 80\%$ is smaller in the $\sigma_r = 200$ km s^{-1} group, $\overline{n}$ is a factor of ∼five times smaller than in NGC 533. As a consequence, the collision timescale for an L^* galaxy in a $\sigma_r = 200$ km s^{-1} group is $\sim 3\times$ longer than for an L^* galaxy in NGC 533.

(d) L_{typ} Galaxy in a $\sigma_r = 200$ km s^{-1} Group. The tidal radius of a typically bright galaxy in a $\sigma_r = 200$ km s^{-1} group is $\sim 45h^{-1}$ kpc, where we assume that the galaxy's velocity dispersion is the same as in case (b). The value of $\overline{n}$ is the same as in case (c). Therefore, T_{col} is $\sim 8\times$ longer in this case than for an L^* galaxy in NGC 533.

Summary. Collision timescales are shortest for bright cluster members, whose cross-sections are large because of the high relative velocities and galaxy number density. T_{col} is increasingly longer for an L^* galaxy in a $\sigma_r = 450$ km s^{-1} group, an L^* galaxy in a $\sigma_r = 200$ km s^{-1} group, an L_{typ} galaxy in a $\sigma_r = 450$ km s^{-1} group, and an L_{typ} galaxy in the lower σ_r group. However, as we will see, the merger timescales do not follow this hierarchy, because they depend not only on the collision timescale, but also on the fraction of collisions that lead to mergers.

3.5.4. Galaxy-Galaxy Merger Timescales

To roughly calculate the merger timescale, we assume that galaxies in collision merge if the ratio of the collision speed to their internal velocity dispersion (σ_g) is ≤ 3 (Tremaine 1980; Richstone & Malumuth 1983). In other words, we determine the fraction of collisions ζ that are slower than $3\sigma_g$. As discussed in Richstone & Malumuth (1983), the fraction of relative velocities in one direction varies as $e^{-\upsilon/4{\sigma_r}^2}$. The merger fraction is then $\zeta = \int_0^{3\sigma_g} e^{-\upsilon^2/4{\sigma_r}^2}\upsilon^2 d\upsilon / \int_0^{\infty} e^{-\upsilon^2/4{\sigma_r}^2}\upsilon^2 d\upsilon$. The merger timescale is thus $T_{merg} = T_{col}\zeta^{-1}$. For an L^* galaxy in NGC 533, $T_{merg} \sim 4T_{col} \sim 0.3t_H$. In contrast, the merger timescale in a rich cluster is $\sim 100\times$ its collision time (Richstone & Malumuth 1983), or about four Hubble times. Thus, T_{merg} for an L^* galaxy is $\sim 13\times$ shorter in NGC 533 than in rich clusters.

For an L_{typ} galaxy in NGC 533, the ratio of the velocity dispersion of the group to that of the galaxy is larger. Therefore, the fraction of collisions that lead to mergers is smaller, and T_{merg} is $11\times$ longer, than for an L^* galaxy. The efficiency of mergers is higher in a $\sigma_r = 200$ km s^{-1} group, because the internal velocity dispersion of an L^* and an L_{typ} galaxy is comparable to σ_r. This effect is somewhat offset by fewer collisions in the lower velocity dispersion group. Therefore, the merger timescale for an L^* and an L_{typ} galaxy is $0.7\times$ and $4\times$ that for an L^* galaxy in NGC 533, respectively.

In summary, the merger timescales are increasingly longer for an L^* galaxy in a $\sigma_r = 200$ km s^{-1} group, an L^* galaxy in a $\sigma_r = 450$ km s^{-1} group, an L_{typ} galaxy in the lower σ_r group, an L_{typ} galaxy in the higher σ_r group, and an L^* galaxy in a rich cluster.

3.5.5. Collisional Stripping Timescale

Even if two colliding galaxies do not merge, the encounter may disrupt their morphologies. The timescale over which mass is removed from a colliding galaxy is shorter in poor groups than in clusters, because the slower relative velocities of the colliding galaxies makes stripping more effective. Numerical experiments (Richstone 1975; Dekel, Lecar, & Shaham 1980; Richstone & Malumuth 1983) suggest that only 1-10% of a galaxy's mass is lost during a collision at velocities typical of galaxies in rich cluster. If we employ the upper bound on the fraction of mass lost, then $T_{strip} \sim 10T_{col}$ is a very rough estimate of the collisional stripping timescale in our highest velocity dispersion groups. Therefore, a collision that is effective at stripping mass from an L^* galaxy in NGC 533 might occur within a Hubble time. More sophisticated simulations are required before this estimate can be improved.

3.5.6. Implications

What do the merger timescales imply for galaxy evolution in poor groups? If $\sigma_r = 450$ km s^{-1} groups like NGC 533 form from the mergers of lower σ_r groups, galaxy-galaxy mergers occur less frequently as the group evolves. In this case, we would expect to observe more on-going galaxy mergers in lower σ_r groups and more merger remnants in higher σ_r groups. In a sample of compact groups with velocity dispersions of order 200 km s^{-1}, a high fraction of galaxies are interacting ($\sim 43\%$; de Oliveira & Hickson 1994). The early type fractions in our $\sigma_r \gtrsim 400$ km s^{-1} groups are as high as in rich clusters. If some early type galaxies are evolved merger remnants, this highly-simplified model is qualitatively consistent with the observed relationship between early type fraction and velocity dispersion, *i.e.,* the galaxy populations of higher velocity dispersion groups are more evolved on average. At some point in the group's evolution, perhaps at a velocity dispersion near 400 km s^{-1}, any morphological evolution resulting from galaxy mergers ceases, and the fraction of merger remnants in poor groups and rich clusters is comparable. The implicit upturn in our $f - \sigma_r$ relation suggests such a saturation point.

Alternatively, the similarity of some group and cluster early type fractions, and the steepening of the $f - \sigma_r$ relationship at high σ_r, might arise from conditions at the time of galaxy formation. For example, it is possible that poor groups such as NGC 533 and rich clusters like Coma begin as similar mass density perturbations with correspondingly similar galaxy populations. In this simple picture, NGC 533 does not develop a cluster-size potential, because its field lacks the surrounding groups that Coma later accretes.

In summary, the cluster-like fraction of early type galaxies in NGC 533, NGC 741, and HCG 62 suggests that the cluster environment is not required to produce copious quantities of E and S0 galaxies. The simplest explanation is either that fluctuations in the initial conditions permitted early types to form in these comparatively low velocity dispersion, low galaxy density environments or that the galaxies' subsequent evolution was the product of a mechanism, such as galaxy-galaxy interactions, common to both groups in the field and groups that become subclusters. Although additional environmental mechanisms may affect the evolution of cluster galaxies, such cluster-specific processes are not required to explain the current data. A cluster that evolves hierarchically from subclusters with the properties of NGC 533, NGC 741, and HCG 62 will have, at least initially, a similar galaxy population. As we demonstrate below, another test of the importance of cluster environment on galaxy evolution at the current epoch is to compare the recent star formation histories of galaxies in poor groups and in subclusters.

3.6. Early-Type Group Galaxies with Young Stellar Populations

3.6.1. Results

The star formation histories of galaxies in poor groups provides additional insight into the environmental factors that may influence the evolution of galaxies. One approach is to examine the spectra of the early types for evidence of on-going star formation or of a young stellar population. We can then compare the fraction of E and S0 group members that have recently formed stars with a sample from rich clusters with complex structure. If early types in poor field groups have different recent star formation histories than those in infalling subclusters, which have only just been exposed to the cluster environment for the first time, then cluster-based galaxy evolutionary mechanisms are clearly potent at the current epoch. On the other hand, if the two samples are similar, then the mechanisms that operate exclusively in clusters or that are much more effective in clusters than in poor groups are not required to enhance and/or quench star formation in these galaxies. In the latter case, recent star formation may be the product of galaxy-galaxy encounters, which are present in both groups and subclusters, or of evolution that is independent of the galaxies' present environment.

To determine which of the E and S0 group members have spectra that indicate on-going or recent star formation, and to compare this population with that in rich, complex clusters, we first automate the calculation of the [O II] λ3727 equivalent width in the manner of Zabludoff *et al.* (1996). The equivalent width uncertainties, which are typically less than 1 Å, are calculated using counting statistics (the detector is a photon counter with approximately zero read noise), the local noise in the continuum, and standard propagation of errors. Figure 8a shows the unfluxed spectra of the central regions of four early type group members with significant [OII] emission (> 5Å, excessive for a normal Sa type galaxy (Kennicutt 1992ab; Caldwell & Rose 1997)). This criterion is the same as that used by Caldwell & Rose (1997) to identify star formation in the spectra of early type galaxies in rich clusters with substructure. However, the ratios of [OIII] λ5007 to Hβ λ4861 and [OII] λ3727 to [OIII] λ5007 suggest that H90_017 is an AGN. Two other spectra in Figure 8a, H42_023 and H62_008, are either star forming or weaker AGN. To be conservative, we include only N741_020 as a star forming galaxy in the subsequent analysis.

Are there early-type group members that have experienced star formation in the last few Gyr and are now quiescent? The ratio of the strength of the Ca II H λ3968 + Balmer Hϵ λ3970 line to the Ca II K λ3934 line is a strong indicator of recent star formation (cf. Leonardi & Rose 1996), especially when there is some filling of the other Balmer absorption lines. We visually identify the spectra of group galaxies with early type morphologies that have H+$H\epsilon$ to K ratios > 1 and signal-to-noise ratios $S/N > 6$. These seven spectra are shown in Figure 8b.

To further test whether the galaxies in Figure 8ab have a young stellar component, we calculate the 4000 Å break D_{4000} for the sample spectra as in Zabludoff *et al.* (1996). The break strength is a measure of the galaxy's color, with lower D_{4000} indicating a bluer stellar population. The eight star forming and post-star forming galaxies in Figure 8ab lie in the blue tail of the D_{4000} distribution (Figure 9, shaded), implying that they have a younger stellar population than is typical for the other early types in the sample (white). The unshaded galaxy blueward of the peak of the shaded subsample is the probable AGN discussed above, H90_017. The case for recent star formation in the shaded subsample is bolstered by stellar population synthesis models (Bruzual & Charlot 1995), which indicate that for a double burst model of star formation in which the second burst lasts a Gyr or less, a galaxy with $D_{4000} \lesssim 2$ has experienced the second burst within the last ~ 2 Gyr, regardless of the assumed initial mass function, burst strength, or progenitor type.

3.6.2. Comparison with Rich Clusters

The star forming and post-star forming galaxies whose spectra are in Figure 8ab are 12% of the 64 early type group members for which we have spectra. How does this fraction compare with that in clusters with infalling groups? Caldwell and Rose (1997) examined galaxy spectra in clusters with significant substructure and found that $\sim 15\%$ of galaxies with early type morphologies have signatures of recent star formation. The resolution of our spectra is $\sim 3\times$ poorer than for that cluster sample, preventing us from precisely duplicating the young stellar population index used by Caldwell and Rose (*e.g.*, their continuum definitions correspond to one pixel or less in our spectra). However, like all of our post-star forming early types, most of the galaxies in Caldwell and Rose's post-starburst sample have sufficiently strong Balmer $H\epsilon$ so that H+$H\epsilon$ EW > K EW (note that Caldwell and Rose include a few possible AGN and transitional S0/a type galaxies of the kind that we exclude from the group sample). Therefore, the fractions of early types with "abnormal" Balmer absorption and/or [OII] emission in poor groups and in subclusters are roughly consistent.

There are two potential problems in comparing the poor group and cluster samples. First, although the spectroscopy of both samples was conducted with fibers of similar size, the physical radius to which the group and cluster galaxies are sampled by the fibers differs, because the Caldwell and Rose systems are generally more distant than ours. This "aperture bias" might alter the apparent contributions of the young and old stellar populations in our our spectra relative to the Caldwell and Rose data. For example, our fibers will tend to miss [OII] emission or Balmer absorption in the outer parts of some E and S0's and to oversample nuclear light in comparison with the Caldwell and Rose spectra. Second, our group sample includes early type galaxies

that are several magnitudes fainter than those in the cluster sample. Although a Kolmogorov-Smirnov test fails to distinguish (at better than the 95% level) between the distributions of estimated absolute magnitude M_B for the early types with and without young stellar populations in our groups, an increase in the fraction of recently star forming galaxies at fainter absolute magnitudes would complicate the comparison of the group and cluster samples.

One way to roughly address these two issues is to compare the Caldwell and Rose data in Coma with our data in NGC 533, because these systems are at similar distances. We cut the NGC 533 sample at the absolute magnitude limits of the Coma sample, $M_B \lesssim -16.6 + 5\log_{10} h$. Three of the 16 galaxies that that we classify as early types have young stellar populations, but no on-going star formation. This fraction of 23% is not significantly different from the fraction of early types with post-starburst spectra in the NGC 4839 subcluster (11/38 = 29%; Caldwell & Rose 1997), whose non-coincident galaxy and X-ray gas distributions suggest that the group is falling into the Coma cluster for the first time (Caldwell *et al.* 1993; White *et al.* 1993a; Zabludoff & Zaritsky 1995). Although the statistics of the samples are poor, it is suggestive that the early type galaxies in NGC 533 have a recent star formation history similar to those in the NGC 4839 subcluster, which has the highest fraction of post-starburst early types of any subclump in a nearby cluster.

The spectra in Figure 8b indicate that some of the early type galaxies in poor groups experienced recent episodes of star formation and are now quiescent. What processes might induce and/or quench star formation in a group galaxy? Mechanisms proposed to deplete gas in rich cluster galaxies include ram pressure stripping (Gunn & Gott 1972), transport processes like viscous stripping and thermal conduction (Nulsen 1982; Cayatte *et al.* 1994), and the expulsion of gas via supernovae-driven winds (cf. Larson & Dinerstein 1975). The tidal limitation of a galaxy's halo by the group potential (§3.3) might also remove gas from a reservoir outside the optical radius. By removing gas from galaxies, these processes are likely to reduce subsequent star formation. Although there are no models at present, it is also conceivable that these mechanisms compress or shock inter-stellar gas, producing an increase in star formation. Because the metallicity of the intra-group gas is poorly known, it is difficult to place strong constraints on the contribution of supernovae ejecta to the intra-group medium. Therefore, we consider only the effects of ram pressure stripping and gas transport processes below.

3.6.3. The Effects of Ram Pressure

It is possible to roughly estimate the ram pressure of the intra-group medium on the inter-stellar medium of group members. Specifically, we estimate the radius r_s at

which the disk of an L^* galaxy is subject to stripping. The condition for stripping for a galaxy that moves with uniform velocity through a uniform intra-group medium is $\rho_{IGM}{v_\perp}^2 > 2\pi G\sigma_{tot}\sigma_{gas}$, where ρ_{IGM} is the density of the intra-group medium, $v_\perp$ is the component of galaxy velocity relative to the intra-group medium that is perpendicular to the disk, σ_{tot} is the surface density of the disk at radius r_s, and σ_{gas} is the surface density of gas in the disk at r_s (Gunn & Gott 1972). This simple condition is consistent with the predictions of n-body/hydrodynamic simulations (Kundić *et al.* 1997). Because NGC 533 has the highest $\rho_{IGM}{v_\perp}^2$ of the 12 groups, we estimate the ram pressure experienced by one of its late type members to obtain a conservative upper limit for the sample.

First we calculate the ram pressure term for a galaxy in the core of NGC 533. We adopt $v_\perp \approx \sqrt{2}\sigma_r = 650$ km s^{-1}. We integrate a King profile (King 1966) of NGC 533's intra-group medium that excludes the central elliptical (Paper II) to obtain an estimate of the central gas density, $\rho_{0,IGM} \sim 2 \times 10^{-3}h$ cm^{-3}. The average gas density within $300h^{-1}$ kpc is then $\overline{\rho_{IGM}} \sim 9 \times 10^{-4}h$ cm^{-3}. Therefore, the ram pressure on a galaxy in the core of NGC 533 is $\overline{\rho_{IGM}}{v_\perp}^2 \sim 4 \times 10^{12}h$ cm^{-1} s^{-2}.

To determine the radius in a disk galaxy at which ram pressure stripping is effective, we calculate where the restoring force pressure $2\pi G\sigma_{tot}\sigma_{gas}$ exceeds the ram pressure. We use the averaged total mass and HI surface density profiles of six nearby, L^* or brighter galaxies from Giovanelli *et al.* (1981) to obtain estimates of σ_{tot} and σ_{gas} at different radii (note that the units in their Figure 7 are mislabelled $M_\odot$ kpc^{-2}, instead of $M_\odot$ pc^{-2}). The exponential scale length of the total mass in the composite disk is ~ 4 kpc. The ram pressure condition is satisfied at $r_s \sim 15$ kpc, or about four scale lengths. This radius is comparable to the furthest extent of optical light in disk galaxies ($\sim$ 3-5 scale lengths; van der Kruit & Searle 1981). As a result, ram pressure will probably not strip gas inside the optical disk of a L^* group member, but may deplete gas if a reservoir exists at larger radii, limiting subsequent star formation by preventing replenishment by infalling gas. It is less likely that ram pressure will affect the morphology of group galaxies, *e.g.*, transforming the bulge-to-disk ratio of a late type spiral into that of an S0.

We note that the estimated central gas density in NGC 533 is comparable to that in Coma, where $\rho_{0,ICM} \sim 5 \times 10^{-3}h^{-1/2}$ cm^{-3} (Hughes 1989). If we assume conservatively that the *average* gas density is the same in groups and clusters, and thus that differences in ram pressure depend only on global velocity dispersion, then galaxies in a $\sigma_r \sim 1000$ km s^{-1} rich cluster experience at least $\sim$ 5-25$\times$ more ram pressure on average than do the members of our groups.

There are several limitations of this estimate of the ram pressure in poor groups. First, the calculation does not include the replenishment by supernovae of gas removed by ram pressure from the outer disk and halo. Second, we assume that gas is uniformly distributed in the disk — any clumping makes the gas harder to strip away because

the stripping force is reduced in proportion to the area of the gas clump, while the gravitational force is unaffected (T. Kundić 1997, priv. comm.). Third, the effects of ram pressure in groups could be enhanced by the tidal tails produced during the collision of two galaxies (see Hibbard *et al.* 1994). The intra-group medium will strip the rarefied gas in the tails more easily than disk gas, perhaps preventing gas from returning to the merger remnant and thereby halting any subsequent star formation. Fourth, we implicitly assume that that the disk surface densities of fainter group members are at least as high as for the L^* galaxy considered here. If the disks of fainter galaxies have substantially lower restoring force pressure, they may be more affected by ram pressure stripping.

3.6.4. The Effects of Viscous Stripping and Thermal Conduction

Transport processes such as viscous stripping and thermal conduction are also proposed as gas removal mechanisms in clusters (Nulsen 1982; Cayatte *et al.* 1994). In contrast to ram pressure stripping, these processes do not depend on the disk's local gravity, except for the most massive and/or slow moving galaxies. Therefore, gas is stripped from the galaxy at all radii, not just from the outermost disk. In addition, gas transport is not sensitive to the orientation of a galaxy with respect to its motion through the intra-group medium, whereas ram pressure depends on the component of the galaxy's velocity perpendicular to its disk. As in the ram pressure calculation above, we assume here that there is no replenishment of the gas once it is swept away and that the galactic gas is uniform. We also assume that ram pressure has not first stripped gas from the disk.

The stripping rate due to gas transport is given by $\dot{M}_t \approx \pi {r_d}^2 \overline{\rho_{IGM}} \upsilon$, where $r_d \sim 30$ kpc is the radius of the gas disk (excluding any ram pressure effects) and $\upsilon \approx \sqrt{2}\sigma_r$ is the approximate velocity of the galaxy through the intra-group medium (Nulsen 1982). For a galaxy within $300h^{-1}$ kpc of the center of NGC 533, the gas mass loss rate is then $\sim 40h\ M_\odot\ \mathrm{yr}^{-1}$. Therefore, a typical galaxy with $\sim 8 \times 10^9 M_\odot$ of HI (NGC 4192 from Cayatte *et al.* 1994) could lose almost 100% of its atomic gas in a crossing time ($t_c/t_H = 0.02$ for NGC 533). However, the HI detected in many poor group members (Giuricin *et al.* 1985) suggests that the effectiveness of this mechanism is overestimated here. As pointed out by Kundić *et al.* (1997), this approximation neglects the formation of a shock in front of the galaxy that prevents some fraction of the intra-group medium from interacting directly with the galactic gas. In addition, the introduction of even a small magnetic field term into the transport equation would limit the effectiveness of the process by reducing the mean free paths of the plasma particles (B. Mathews 1997, priv. comm.). An improved understanding of the significance of gas transport mechanisms in groups awaits detailed simulations. As in

the case of ram pressure, gas transport may limit the subsequent star formation of the galaxy, but the requirements for transforming the galaxy into an earlier morphological type, *e.g.*, the total disruption of the stellar disk or an increase in the bulge-to-disk ratio, are not part of this picture.

3.6.5. Implications

In the preceding discussion, we demonstrated that the effects of ram pressure stripping are weaker in poor groups than in rich clusters. We suggested that, even if gas disruptive processes like ram pressure stripping, viscous stripping, or thermal conduction can induce star formation as well as truncate it, they are unlikely to significantly affect the stellar morphology of a galaxy. Therefore, if one environmental mechanism is responsible for both the high early type fractions of some poor groups and the young stellar populations of certain early type group galaxies, galaxy-galaxy encounters provide a possible explanation. Such interactions can produce bursts of star formation (*e.g.*, Londsdale *et al.* 1984; Kennicutt *et al.* 1987; Sanders *et al.* 1988) in which the gas is consumed or stripped away.

Although our observations of poor groups suggest that the effects of cluster environment are not required to produce the early type fractions and star formation episodes of nearby clusters, we suspect that the star formation histories of group and subcluster galaxies will begin to deviate after the subclump and cluster mix. Proposed gas removal processes including ram pressure stripping, the tidal limitation of galaxy halos, and galaxy harassment, which are more efficient in clusters than in groups, may eventually suppress star formation in cluster galaxies. Comparative studies of the HI content of field, group, and cluster galaxies will help to resolve this issue.

4. Conclusions

We use fiber spectroscopy to obtain 963 galaxy redshifts in the fields of 12 poor groups of galaxies. When combined with 39 redshifts from the literature, the survey consists of 1002 galaxy redshifts, 280 of which are group members. The groups have mean recessional velocities between 1600 and 7600 km s^{-1}. Nine groups, including three Hickson compact groups, are detected in X-rays by ROSAT (Paper II). Our conclusions are the following:

1. Remarkably, there are at least $\sim$ 20-50 group members to absolute magnitudes as faint as $M_B \sim -14$ to $-16 + 5\log_{10} h$ in each of the X-ray-detected groups, most of which were previously known as groupings of less than five bright ($\lesssim M_B{}^*$) galaxies (§3.1, Figure 2). The large number of group members, the significant early-type

populations (up to $\sim 55\%$ of the membership) and their concentration in the group centers, the short crossing times (less than 0.05 of a Hubble time) through a massive, common halo (see point 2 below), and the correspondence of the central, giant elliptical with the optical and X-ray group centroids argue that the X-ray detected groups are bound systems, not chance superpositions of unbound galaxies along the line-of-sight, and that the cores of these groups are close to virialization or virialized. An exception is HCG 90, a dynamically evolving group whose several core galaxies appear to be interacting (Longo *et al.* 1994) and whose asymmetric X-ray emission is not coincident with any of the bright group members.

Because we increase the membership by a factor of 10 in many of our groups, we can, for the first time, determine poor group velocity dispersions with sufficient precision ($\lesssim 20\%$) that the differences among them are statistically meaningful (§3.2). The velocity dispersions of the X-ray groups range over more than a factor of two, from 190 km s^{-1} in HCG 90 and 210 km s^{-1} in HCG 42 to 430 km s^{-1} in NGC 741 and 460 km s^{-1} in NGC 533. We are now quantifying the baryonic contribution of the faint group members which, when coupled with our improved group velocity dispersion determinations, will allow us to place better constraints on the baryon fraction of poor groups.

The non-X-ray-detected groups have lower velocity dispersions (< 130 km s^{-1}) and early-type fractions ($= 0\%$) than the X-ray groups. We are unable to determine whether any of the three non-X-ray groups in our sample are bound systems with little or no X-ray gas or whether they are all just superpositions of unbound galaxies along the line-of-sight. It is important to note that the Local Group, a system collapsing for the first time (cf. Zaritsky 1994), would appear to have optical properties similar to the non-X-ray groups if it were moved to their distances.

2. The group velocity dispersion does not decrease significantly from the center out to the virial radius (typically $\sim 0.5h^{-1}$ Mpc), implying that the mass in the group is extended (§3.3, Figure 5). The mass of the group halo (~ 0.5-$1 \times 10^{14}h^{-1}M_{\odot}$) is large compared with that of the X-ray gas ($\sim 1 \times 10^{12}h^{-5/2}M_{\odot}$) and of the galaxies ($\sim 1 \times 10^{13}h^{-1}\ M_{\odot}$), whose individual halos may have been tidally-limited by the group potential at the time of the system's formation (Merritt 1984) or subsequently reduced by collisional stripping (Richstone 1975; Dekel, Lecar, & Shaham 1980). The small fraction of the group mass associated with the galaxies may slow the rate at which they interact (Governato *et al.* 1991; Bode 1993; Athanassoula 1997), allowing the group to virialize before all of its members merge and to exist as a group for more than a few crossing times. This picture is further supported by the evidence, described in point 1 above, that the cores of some poor groups have survived long enough to virialize and by the X-ray observations discussed in Paper II.

3. The giant, brightest elliptical in each X-ray group (a galaxy that lies within ~ 5-$10h^{-1}$ kpc of the X-ray center, Paper II) occupies a position that is indistinguishable,

in radial velocity and on the sky, from the center of the group potential (§3.4, Figure 6). This result suggests that dominant cluster ellipticals, such as "cD" galaxies (Matthews, Morgan, & Schmidt 1965), may form via the merging of other galaxies in the centers of poor group-like environments (*e.g.,* Hickson compact group 90), perhaps during the initial collapse of the group when the conditions for galaxy capture are most favorable (Merritt 1985). The similarity of the velocity dispersions of the group and the central elliptical may allow the BGG to subsequently grow through mergers with bound companions, with slow-moving galaxies on radial orbits, or with galaxies that fall into the core via dynamical friction (depending on the group, an L^* galaxy at a radius of $\sim$ 250-400h^{-1} kpc would fall to the center in a Hubble time; see Merritt 1984). Groups with a central, dominant elliptical may then fall into richer clusters (Merritt 1985). This scenario explains why cD's do not always lie in the spatial and kinematic center of rich clusters (Zabludoff *et al.* 1990; Dunn 1991; Zabludoff *et al.* 1993), but instead occupy the centers of subclusters in non-virialized clusters (Geller & Beers 1983; Bird 1994; Beers *et al.* 1995).

4. The fraction of early-type galaxies in poor groups varies significantly (§3.5, Figure 7), ranging from that characteristic of the field ($\lesssim 25\%$) to that more consistent with rich clusters ($\sim 55\%$). The high early type fractions of groups like NGC 533, NGC 741, and HCG 62 are particularly surprising, because all the 12 sample groups have substantially lower velocity dispersions (a factor of $\sim$ 2-5) and galaxy number densities (a factor of $\sim$ 5-20) than are typical of rich clusters. What environmental factors might be responsible for the high early type fractions in these three groups? First, the effects of disruptive mechanisms like galaxy harassment (Moore *et al.* 1996; B. Moore 1997, priv. comm.) on the morphologies of poor group galaxies are weaker than in cluster environments. Second, although the tidal limitation of group member halos, the expulsion of gas by supernovae-driven winds, the ram pressure stripping of gas in the outermost disk, or the removal of gas due to turbulent viscous stripping and thermal conduction may reduce the galaxies' gas reservoirs and thus limit their star formation, these processes are unlikely to affect galaxy morphology (*e.g.*, it is hard to transform the bulge-to-disk ratio of a late type spiral into that of an S0 galaxy). Third, strong gravitational shocks generated as galaxies pass near the core on radial orbits might tidally transform some Sc-Sd galaxies into dwarf ellipticals (B. Moore 1997, priv. comm.), but only four of the 72 galaxies in our early type sample are as faint as dE/dSph's (*i.e.,* $M_B \gtrsim -16 + 5\log_{10}\ h$).

In contrast, the kinematics of poor groups make them favorable sites for galaxy-galaxy encounters (Barnes 1985; Aarseth & Fall 1980; Merritt 1985), even though the partial truncation of the galaxy halos acts to reduce the frequency of such interactions. Mechanisms such as tidal collisions and mergers may influence the morphologies and star formation histories of some group galaxies. Another possible explanation of the cluster-like early type fractions of some poor groups is that environment is relatively

unimportant at late times and that conditions during the epoch of galaxy formation dominate.

5. The fraction of early-type group members that have spectral evidence of on-going or recent star formation in their central regions (at least 12%; §3.6, Figures 8-9) is consistent with that seen in rich clusters with significant substructure ($\sim 15\%$; Caldwell & Rose 1997). If some of the subclusters in these complex clusters are groups that have recently fallen into the cluster environment for the first time, the similarity between the star formation histories of the early types in the subclusters and of those in our sample of field groups implies that the cluster environment and processes such as ram pressure stripping (Gunn & Gott 1972) are not required to enhance and/or quench star formation in these particular galaxies. If the recent star formation is tied to the external environment of the galaxies and not to internal perturbations, this result is consistent with the picture in which the star formation histories of some early type galaxies are influenced by recent (within the last $2h^{-1}$ Gyr) galaxy-galaxy encounters.

In future papers, we will discuss the relationships between the X-ray and optical properties of these groups (Paper II), the form of the group galaxy luminosity function, and the baryon fractions of poor groups.

We thank Dennis Zaritsky, Lars Hernquist, and Richard Mushotzky for important insights and detailed comments on the text, Allan Sandage for help with the art of galaxy classification, and Arif Babul, George Blumenthal, Michael Bolte, Jack Burns, David Burstein, Tomislav Kundić, Bill Mathews, Ben Moore, Julio Navarro, David Schiminovich, David Spergel, Jacqueline van Gorkom, and Steven Zepf for interesting and useful conversations. AIZ acknowledges support from the Carnegie and Dudley Observatories, the AAS, NSF grant AST-95-29259, and NASA grant HF-01087.01-96A. JM acknowledges support provided by NASA grant NAG 5-2831 and NAG 5-3529.

Table 1: Galaxy Data (Example)

Galaxy	α			δ			v	δv	line	type	plate/	ref
	2000.0						km s^{-1}				CCD	
...												
N533_009	1	24	14.8	1	2	56	5521	80	0	s	p	
N533_035	1	24	17.8	2	21	21	4888	80	2	s	p	
N533_114	1	24	19.3	2	12	1	36710	80	0	...	...	
N533_022	1	24	22.8	1	45	0	5311	80	0	e	p	
N533_032	1	24	24.0	1	38	33	5026	80	0	e	p	
N533_119	1	24	24.2	1	36	37	27833	80	1	...	...	
N533_038	1	24	26.7	2	13	58	11662	80	0	...	...	
N533_014	1	24	28.7	1	8	20	9168	80	0	...	...	N
N533_020	1	24	32.8	2	0	8	5533	80	0	s	p	
N533_001	1	24	33.8	1	43	53	5007	80	0	s	c	
N533_005	1	24	36.4	2	2	39	9601	80	0	...	...	
N533_107	1	24	37.2	1	50	15	32854	80	1	...	...	
...												

Table 2: Group Kinematic Properties

Group	α			δ			N_{tot}	N_{grp}	$\overline{v}$	σ_r	r_{samp}	r_p	r_h	M_{vir}	t_c/t_H
	2000.0								km s^{-1}			h^{-1} Mpc		h^{-1} M$_\odot$	
NGC 533	1	25	29.1	+01	48	17	99	36	5422 ± 81	464 + 58, − 52	0.69	0.59	0.42	1×10^{14}	0.02
NGC 741	1	57	00.7	+05	40	00	82	41	5555 ± 71	432 + 50, − 46	0.70	0.55	0.39	1×10^{14}	0.02
NGC 2563	8	20	24.4	+21	05	46	49	29	4900 ± 67	336 + 44, − 40	0.62	...	...	...	...
HCG 42	10	00	13.1	−19	38	24	106	22	3828 ± 52	211 + 38, − 34	0.49	...	...	...	...
NGC 4325	12	23	18.2	+10	37	19	68	18	7558 ± 70	265 + 50, − 44	0.95	0.51	0.40	4×10^{13}	0.04
HCG 62	12	52	57.9	−09	09	26	106	45	4385 ± 59	376 + 52, − 46	0.56	...	...	...	...
NGC 5129	13	24	36.0	+13	55	40	85	33	6971 ± 56	294 + 43, − 38	0.88	0.71	0.56	7×10^{13}	0.05
NGC 5846	15	05	47.0	+01	34	25	52	20	1892 ± 89	368 + 72, − 61	0.24	...	...	...	...
HCG 90	22	02	31.4	−32	04	58	75	16	2545 ± 58	193 + 36, − 33	0.33	...	...	...	...
NGC 491	1	21	08.7	−34	07	49	104	6	3786 ± 66	86 +117, − 67	0.48	...	...	...	...
NGC 664	1	44	02.7	+04	19	02	67	6	5399 ± 80	130 +244, − 99	0.68	0.57	0.33	8×10^{12}	0.07
N7582	23	18	54.5	−42	18	28	109	8	1612 ± 46	38 + 37, − 36	0.21	...	...	...	...

References

Aarseth, S.J. & Fall, S.M. 1980, ApJ, **236**, 43

Athanssoula, E. 1997, preprint.

Bahcall, N. 1977, ARA & A, **2**, 505

Bahcall, N. 1975, ApJ, **198**, 249

Barnes, J. 1989, Nature, **338**, 123

Barnes, J. 1985, M.N.R.A.S., **215**, 517

Beers, T., Flynn, K., & Gebhardt, K. 1990, AJ, **100**, 32

Beers, T., Kriessler, J., Bird, C., & Huchra, J. 1995, AJ, **109**, 874

Beers, T. & Geller, M. 1983, ApJ, **274**, 491

Binney, J. & Tremaine, S. 1987, in *Galactic Dynamics*, (Princeton: Princeton University Press)

Bird, C. 1994, AJ, **107**, 1637

Blumenthal, G., Faber, S., Flores, R., & Primack, J. 1986, ApJ, **301**, 27

Bode, P.W., Berrington, R.C., Cohn, H.N., & Lugger, P.M. 1994, ApJ, **433**, 479

Bode, P.W., Cohn, H.N., & Lugger, P.M. 1993, ApJ, **416**, 17

Bothun, G., Geller, M., Beers, T., & Huchra, J. 1983, ApJ, **268**, 47

Bruzual, A.G., & Charlot, S. 1993, ApJ, **405**, 538

Caldwell, N. & Rose, J. 1997, AJ, **113**, 492

Caldwell, N. Rose, J.A., Sharples, R.M., Ellis, R.S., & Bower, R.G. 1993, AJ, **106**, 473

Cayatte, V., Kotanyl, C., Balkowski, C., & van Gorkom, J.H. 1994, AJ, **107**, 1003

Danese, L., de Zotti, G., & di Tullio, G. 1980, A & A, **82**, 322

de Calvalho, R., Ribeiro, A., & Zepf, S. 1994, ApJS, **93**, 47

Dekel, A., Lecar, M., & Shaham, J. 1980, ApJ, **241**, 946

de Oliveira, C.M. & Hickson, P. 1994, ApJ, **427**, 684

Diaferio, A., Geller, M., & Ramella, M. 1995, AJ, **109**, 2293

Dressler, A. 1978, ApJ, **226**, 55

Dunn, A. 1991, in *Clusters and Superclusters of Galaxies*, Contributed Talks and Poster Papers, NATA Advanced Study Institute, Institute of Astronomy, Cambridge, eds. Colless, Babul, Edge, Johnstone, & Raychaudhury, p.13

Evrard, A., Metzler, C., & Navarro, J. 1996, ApJ, **469**, 494

Faber, S. & Jackson, R. 1976, ApJ, **204**, 668

Forbes, D. & Thomson, R. 1992, M.N.R.A.S., **254**, 723

Giovanelli, R., & Haynes, M.P. 1985, ApJ, **292**, 404

Governato, F., Bhatia, R., & Chincarini, G. 1991, ApJL, **371**, L15

Gunn, J. 1977, ApJ, **218**, 592

Gunn, J.E., & Gott, J.R. 1972, ApJ, **176**, 1

Helou, G., Madore, G., Schmitz, M., Bicay, M., Wu, X. & Bennett, J. 1991, in "Databases and On-Line Data in Astronomy," ed. D. Egret & M. Albrecht (Dordrecht: Kluwer), p. 89.

Hernquist, L., Katz, N. & Weinberg, D. 1995, ApJ, **442**, 57

Hibbard, J.E., Guhathakurta, P., van Gorkom, J.H., & Schweizer, F. 1994, AJ, **107**, 67

Hickson, P., de Oliveira, M., Huchra, J., & Palumbo, G. 1992, ApJ, **399**, 353

Hickson, P., Huchra, J., & Kindl, E. 1988, ApJ, **331**, 64

Hickson, P. 1982, ApJ, **255**, 382

Huchra, J.P., Geller, M.J., & Corwin, H. 1995, ApJS, **99**, 391

Hughes, J. 1989, ApJ, **337**, 21

Hunsberger, S., Charlton, J., & Zaritsky, D. 1996, ApJ, **462**, 50

Jarvis, J.F. & Tyson, J.A. 1981, AJ, **86**, 476

Kennicutt, R.C., Roettiger, K.A., Keel, W.C., Van der Hulst, J.M. & Hummel, E. 1987, ApJ, **93**, 1011

Kennicutt, R.C. 1992a, ApJS, **79**, 255

Kennicutt, R.C. 1992b, ApJ, **388**, 310

King, I. 1972, ApJL, **174**, L123

King, I. 1966, AJ, **71**, 64

Kirshner, R., Oemler, A., Schechter, P., & Shectman, S. 1983, AJ, **88**, 1285

Kormendy, J. & Bender, R. 1996, ApJ, **464**, 119

Kundić, T., Hernquist, L., & Spergel, D. 1997, preprint

Larson, R.B. & Dinerstein, H.L. 1975, PASP, **87**, 911

Leonardi, A. & Rose, J. 1996, AJ, **111**, 182

Lin, H. 1995, Ph.D. Thesis, Harvard University

Lonsdale, C.J., Persson, S.E., & Matthews, K. 1984, ApJ, **287**, 95

Longo, G., Busarello, G., Lorrenz, H., Richter, G., & Zaggia, S. 1994, A & A, **282**, 418

Maddox, J., Efstathiou, G.; Sutherland, W. J.; Loveday, J. 1990, M.N.R.A.S., **243**, 692

Mamon, G.A. 1992, in *Physics of Nearby Galaxies: Nature or Nurture?*, ed. T.X.

Thuan, C. Balkowski, & J. Tran Thanh Van, 12th Moriond Astrophysics Meeting (Gif-sur-Yvette: Editions Frontières), p.367

Matthews, T.A., Morgan, W.W., & Schmidt, M. 1965, in *Quasi-Stellar Sources and Gravitational Collapse*, eds. Robinson, Schild, and Schucking (Chicago: University of Chicago Press), p.105

McElroy, D.B. 1995, ApJS, **100**, 105

Merritt, D. & Tremblay, B. 1996, AJ, **111**, 2462

Merritt, D. 1985, ApJ, **289**, 18

Merritt, D. 1984, ApJ, **276**, 26

Mink, D. J. & Wyatt, W. F. 1995, Astronomical Data Analysis Software and Systems IV, ASP Conference Series, Vol. 77, 1995, R.A. Shaw, H.E. Payne, and J.J.E. Hayes, eds., p. 496.

Moore, B., Katz, N., Lake, G., Dressler, A., & Oemler, A. 1996, Nature, **379**, 613

Mulchaey, J. S. & Zabludoff, A.I. 1997, ApJ, submitted. (Paper II)

Mulchaey, J. S., Davis, D. S., Mushotzky, R. F. & Burstein, D. 1993, ApJL, **404**, L9

Mulchaey, J. S., Mushotzky, R. F., Burstein, D. & Davis, D. S. 1996a, ApJL, **456**, L5

Mulchaey, J., Davis, D., Mushotzky, R., & Burstein, D. 1996b, ApJ, **456**, 80

Navarro, J.F., Frenk, C.S., & White, S.D.M. 1996, ApJ, **462**, 563

Oemler, A. 1992, in *Clusters and Superclusters of Galaxies*, ed. A.C. Fabian (Dordrecht: Kluwer), p.29

Nulsen, P. 1982, M.N.R.A.S., **198**, 1007

Ostriker, J., Lubin, L., & Hernquist, L. 1995, ApJ, **444**, 61

Peebles, P.J.E. 1970, AJ, **75**, 13

Pildis, R., Bregman, J., & Evrard, A. 1995, ApJ, **443**, 514

Ponman, T., Bourner, P., Ebeling, H., & Bohringer, H. 1996, M.N.R.A.S., **283**, 690

Ponman, T. & Bertram, D. 1993, Nature, **363**, L51

Ramella, M., Geller, M.J., & Huchra, J.P. 1989, ApJ, **344**, 57

Richstone, D. & Malumuth, E. 1983, ApJ, **268**, 30

Richstone, D. 1975, ApJ, **200**, 535

Rose, J.A. 1977, ApJ, **211**, 311

Rubin , V., Hunter, D., & Ford, W. 1991, ApJS, **76**, 153

Sanders, D.B., Soifer, B.T., Elias, J.H., Matthews, K., & Madore B.F. 1988, ApJ, **325**, 74

Schechter, P.L. 1976, ApJ, **203**, 297

Schombert, J. 1988, ApJ, **328**, 475

Schweizer, F. & Seitzer, P. 1992, AJ, **104**, 1039

Schweizer, F. 1986, Science, **231**, 227

Shectman, S.A., Schechter, P.L., Oemler, A.A., Tucker, D., Kirshner, R.P., & Lin, H. 1992, in Clusters and Superclusters of Galaxies (ed. Fabian, A.C.) 351-363 (Kluwer, Dordrecht)

Shectman, S.A., Landy, S.D., Oemler, A., Tucker, D.L., Lin, H., Kirshner, R.P.; Schechter, P.L. 1996, ApJ, **470**, 172

Trager, S.C. 1997, Ph.D. Thesis, University of California, Santa Cruz.

Tremaine, S. 1990, in *Dynamics and Interactions of Galaxies*, ed. Wielen (Berlin: Springer-Verlag), p.394

Tonry, J. & Davis, M. 1981, ApJ, **246**, 680

van den Bergh, S. 1992, A & A, **264**, 75

van der Kruit, P. & Searle, L. 1981, A & A, **95**, 105

Weil, M. & Hernquist, L. 1996, ApJ, **460**, 101

White, S., Briel, U., & Henry, P. 1993, M.N.R.A.S., **261**, L8

Whitmore, B., Gilmore, D., & Jones, C. 1993, ApJ, **407**, 489

Yahil, A. & Vidal, N. 1977, ApJ, **214**, 347

Yun, M.S., Verdes-Montenegro, L., del Olmo, A., Perea, J. 1997, ApJ, **475**, 21

Zabludoff, A.I. & Zaritsky, D. 1995, ApJL, **447**, L21

Zabludoff, A.I., Huchra, J.P., Geller, M.J., & Vogeley, M.S. 1993, AJ, **106**, 1273

Zabludoff, A.I., Huchra, J.P., & Geller, M.J. 1990, ApJS, **74**, 1

Zaritsky, D., Smith, R., Frenk, C., & White, S. 1997, ApJ, **478**, 39

Zaritsky, D., Zabludoff, A.I., & Willick, J. 1995, AJ, **110**, 1602

Zaritsky, D. & White, S. 1994, ApJ, **435**, 599

Zaritsky, D. 1994, in *The Local Group: Comparative and Global Properties*, eds. A. Layden, R. C. Smith, and J. Storm, ESO Conference and Workshop Proceedings No. 51, p.187

Zepf, S. & Whitmore, B. 1993, ApJ, **418**, 72

Figure Captions

Figure 1: The residuals of the heliocentric velocities from this paper and HI velocities from the literature (NASA Extragalactic Database (NED), Helou *et al.* 1991) vs. our internal velocity error estimates for 39 galaxies. The mean residual of 13 km s^{-1} (solid line) is small compared with the *rms* deviation of the residuals (83 km s^{-1}) and is consistent with the mean velocity of 94 stars (-17 km s^{-1}) that were serendipitously observed with the same instrument (dashed line). Therefore, we do not apply a zero-point correction to the galaxy velocities. We adopt 80 km s^{-1} as an estimate of the true velocity error in cases where the internal error is smaller than 80 km s^{-1}. This error estimate is consistent with the average external error estimate of $\sim$70 km s^{-1} for the Las Campanas Redshift Survey (Shectman *et al.* 1996), which employed the same fiber spectrograph setup.

Figure 2: Galaxy velocity distributions from 0 to 30000 km s^{-1} for the 12 poor groups in our sample. The first nine groups are detected by the ROSAT PSPC, the last three are not (Paper II). Note that other groups or richer clusters are detected in many of the group fields. The shaded histograms indicate the N_{grp} group members identified with the 3σ-clipping algorithm described in §3.1. Because each field is sampled to a different absolute magnitude limit and out to a different physical radius, the histograms do not precisely reflect the actual differences in group galaxy number densities (see §3.1 and Figure 4). The histograms do reveal large populations of group members down to absolute magnitudes of $M_B \sim -14$ to $-16 + 5\log_{10}\ h$.

Figure 3: The projected spatial distributions of the members of the 12 sample groups. The total angular size of each plot is 1.62×1.62 degrees, slightly larger than the fiber spectrograph field of 1.5×1.5 degrees. Digitized scans of Palomar Sky Survey or UK Schmidt plates (APM Survey (Maddox *et al.* 1990); STScI Digitized Sky Survey) are not complete for every group; hence, we observe no galaxies in the westernmost fifth of the NGC 741 field, in the northernmost fifth of the NGC 5129 field, in the northernmost fifth of the HCG 90 field, and the northernmost tenth of the NGC 7582 field (as indicated by the dashed lines). The galaxies are typed to an apparent magnitude of $m_B \sim 17$. Early type galaxies (E, S0) are denoted by "0", late type galaxies (non-E, non-S0) by "S". The filled circles mark the untyped group members. The scale bar below each group name is $0.3h^{-1}$ Mpc. The early types tend to be more concentrated in the group centers than the late types.

Figure 4: The number of group galaxies within a projected radius of $0.3h^{-1}$ Mpc and with absolute magnitudes of $M_B \lesssim -17 + 5\log_{10}\ h$. The observed number counts of members within these limits are shaded. To roughly compensate for incomplete sampling down to the magnitude limit (completeness is indicated by the fraction above each histogram bar), we assume that the fraction of all unobserved galaxies that are group members is the same as the fraction of all observed galaxies that are members.

The white histogram shows these "corrected" group galaxy counts. Magnitude errors introduce more uncertainty into the "corrected" galaxy counts (see §3.1), so a small difference between the counts of two groups is not significant. Nevertheless, this plot shows that the trend is for non-X-ray-detected groups to have lower galaxy densities than are typical of X-ray groups. For the same radial and magnitude cuts, the Coma cluster (NED) has 83 members (a lower limit because we make no correction for incompleteness), implying that its galaxy density is $\sim$ 5-20$\times$ that of the poor groups.

Figure 5: The velocity offset vs. the projected radial offset of 204 X-ray group members from the central, giant elliptical (BGG) in each group. The velocity offset is normalized with the internal velocity dispersion of the BGG (σ_{BGG}). We plot only the seven X-ray groups for which σ_{BGG} is known (HCG 42, HCG 90, NGC 2563, NGC 5129, NGC 5846, NGC 533, NGC 741). We calculate the normalized velocity dispersion (δ) (i.e., the *rms* deviation in the normalized velocity offset) within each radial bin (dashed lines). We show the magnitude of δ as a scale bar at the bottom of each bin. The first bin ($0 < r \leq 100h^{-1}$ kpc; 47 galaxies) has $\delta = 1.3$, the second ($100 < r \leq 200h^{-1}$ kpc; 40 galaxies) has $\delta = 1.4$, the third ($200 < r \leq 300h^{-1}$ kpc; 34 galaxies) has $\delta = 1.4$, the fourth ($300 < r \leq 500h^{-1}$ kpc; 43 galaxies) has $\delta = 1.3$, and the fifth ($500 < r \leq 1000h^{-1}$ kpc; 40 galaxies) has $\delta = 1.3$. The differences in δ with radius are not statistically significant. The flatness of the δ profile to at least $\sim 0.5h^{-1}$ Mpc, in contrast to the factor of two decrease expected for a Keplerian system, suggests that the group galaxies move through a common dark halo. In all bins, $\delta > 1$, which shows that matter is dynamically cooler in the BGG than in the surrounding group.

Figure 6: (a) The kinematic (y) and projected spatial (x) offsets of the central, giant elliptical (filled squares) and other group members (filled circles) from the group centroid for the nine X-ray groups. The velocity offset of each galaxy from the mean velocity of the group is divided by the group velocity dispersion σ_r to compensate for differences in the size of the group global potentials. The y errorbars represent the 68% confidence limits on y obtained from adding the errors in the group mean velocity and the BGG velocity in quadrature. To estimate the 68% error in x for a BGG in a group with N_{grp} members, we use a statistical jackknife test in which samples of N_{grp} galaxies are drawn from HCG 62, the group with the most members. For each BGG, we adopt the *rms* deviation in the distribution of x (ϵ_x) for these samples as the x error. (For the BGG in HCG 62, we use the smallest x error calculated among the other groups). Note that the incomplete, asymmetric spatial sampling of the fiber field in NGC 741 and NGC 5129 (see Figure 3) contribute to their high x values and that their x errors are consequently underestimated here. (b) The distributions of the statistic R (see text) for all of the group members (solid) and for the subset of BGGs (shaded). A galaxy that has a large peculiar motion and/or that lies outside the projected group core has a larger R value than a galaxy at rest in the center of the group potential. A Student's t-test gives $< 3 \times 10^{-5}$ as the probability that the means

of the non-BGG and BGG distributions are consistent. The heavy line shows the distribution of R obtained by assuming that all of the BGG's lie in the centers of their groups. A t-test fails to differentiate between the means of the model R distribution and that of the BGGs (shaded) at better than the 95% confidence level. We conclude that (1) the BGG's are significantly more concentrated than the other group members and (2) to within the errors, the BGG's occupy the center of the group potential.

Figure 7: Histogram of the early type (E, S0) fractions of the 12 sample groups. Note that the ∼55% fractions for three X-ray groups, HCG 62, NGC 741, and NGC 533, are consistent with the early type fractions typical for rich clusters over similar radii (0.5-1.0h^{-1} Mpc; Whitmore, Gilmore, & Jones 1993). The early type fractions in these three poor groups are inconsistent with those of groups like NGC 2563, which have morphological populations characteristic of the field (∼30%; Oemler 1992). Of the 6-8 group members found in the three non-X-ray groups (shaded), we find no early types. The inset shows the correlation between early type fraction f and group velocity dispersion σ_r for the 12 sample groups. The solid line is an unweighted fit to the data, the dashed line is a fit weighted by the velocity dispersion errors. In both cases, the correlation is significant at the > 0.999 level, implying either that galaxy morphology is set by the local potential size at the time of galaxy formation (Hickson, Huchra, & Kindl 1988) and/or that σ_r and f increase as a group evolves (Diaferio *et al.* 1995).

Figure 8: (a) Observed, unfluxed spectra of the central regions of four early type group members with significant [OII] emission (> 5Å). The spectra are smoothed to 1.5× the instrument resolution of 5-6Å. The scale bar to the left of each spectrum is 50 counts. (b) Spectra of the central regions of seven early type group members for which the Ca II H+$H\epsilon$ line is stronger than the Ca II K line. The spectrum of N741_020 in (a) and the post-star formation spectra in (b) comprise 12% of the sample of 64 early type group members for which we have spectra. This fraction of star forming and post-star forming early type galaxies is consistent with that typical of rich clusters with significant substructure (∼ 15%; Caldwell & Rose 1997).

Figure 9: Distributions of the 4000Å break D_{4000} for the early type group members (white) and for the subset of eight star forming and post-star forming galaxies in Figure 8 (shaded). The subsample clearly consists of bluer galaxies (the blue galaxy not included in the subsample is an AGN, H90_017). The combination of small D_{4000} and large Ca II H+$H\epsilon$ to Ca II K ratio indicates that the subsample galaxies have younger stellar populations than are typical for early type galaxies in poor groups. (Note that this distribution of D_{4000} is not directly comparable to that of the Las Campanas Redshift Survey (LCRS; Zabludoff *et al.* 1996), because the falling detector response in the blue for our lower redshift group sample causes a steepening (reddening) of the 4000Å break relative to the more distant field sample drawn from the LCRS.)

Fig. 1.—

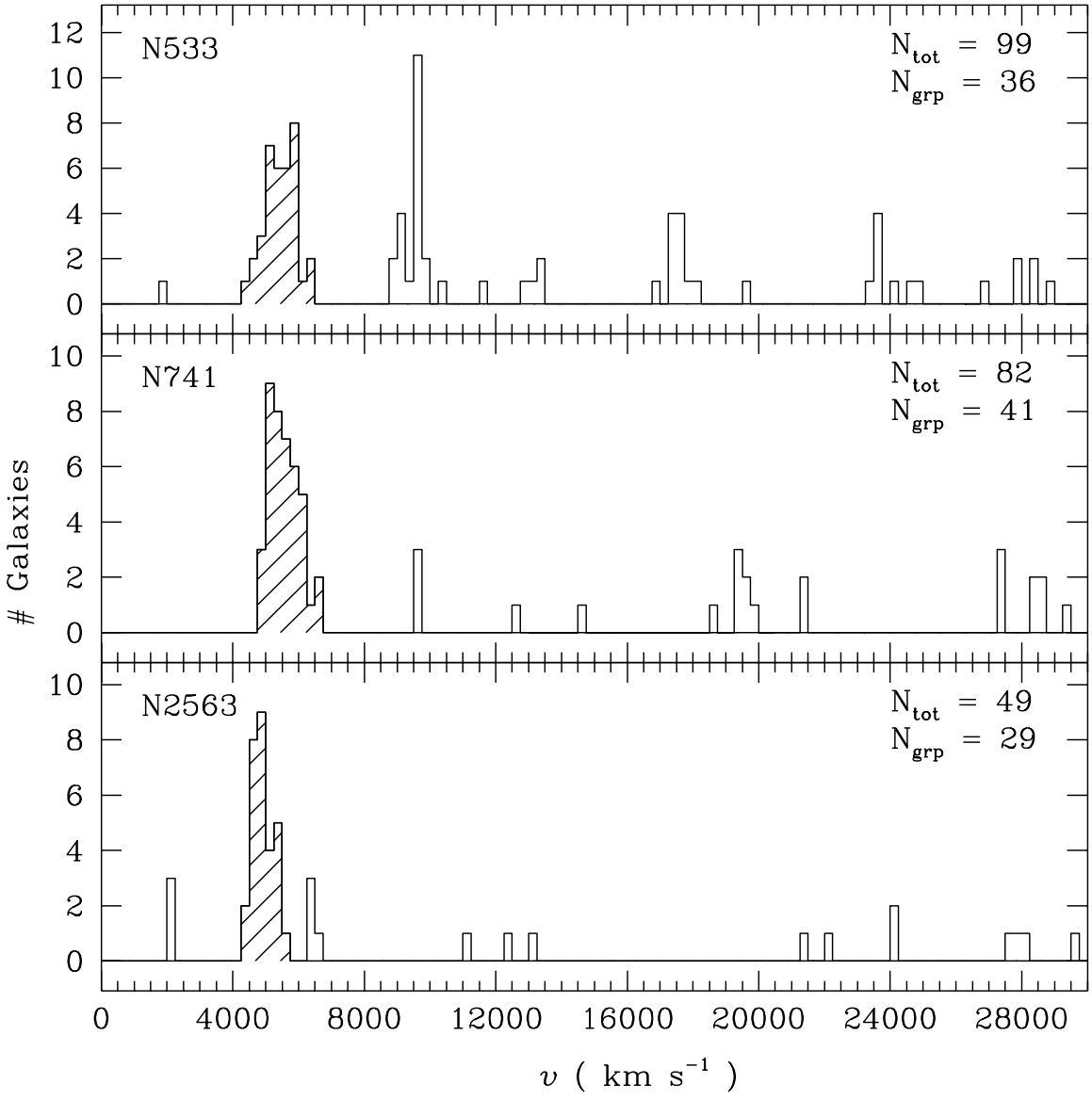
N533
N_tot = 99
N_grp = 36
N741
N_tot = 82
N_grp = 41
N2563
N_tot = 49
N_grp = 29
# Galaxies
v (km s^-1)
0
4000
8000
12000
16000
20000
24000
28000

Fig. 2.—

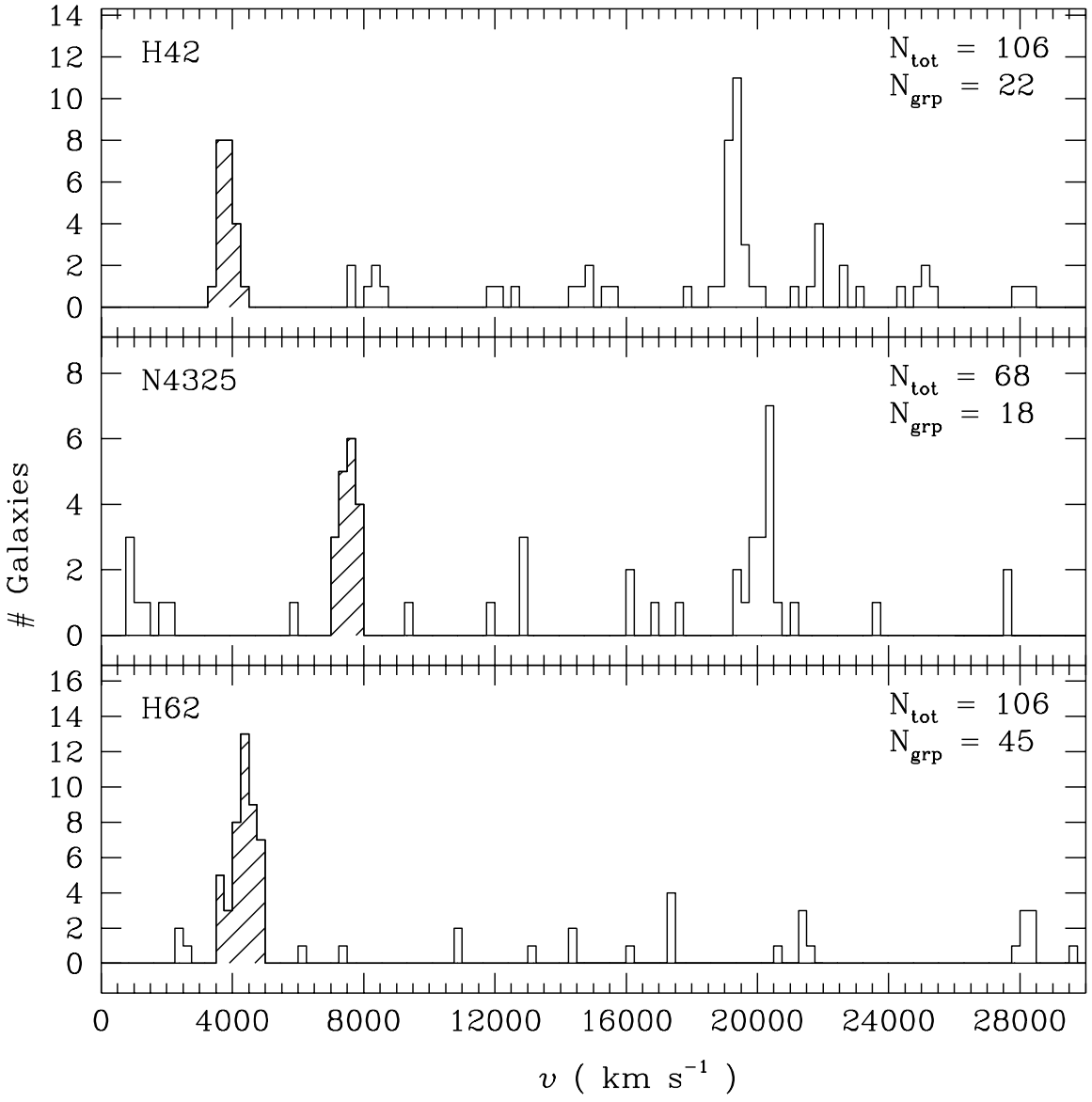
H42
N_tot = 106
N_grp = 22
N4325
N_tot = 68
N_grp = 18
H62
N_tot = 106
N_grp = 45
# Galaxies
v (km s^-1)
0
4000
8000
12000
16000
20000
24000
28000

Fig. 2.— *cont.*

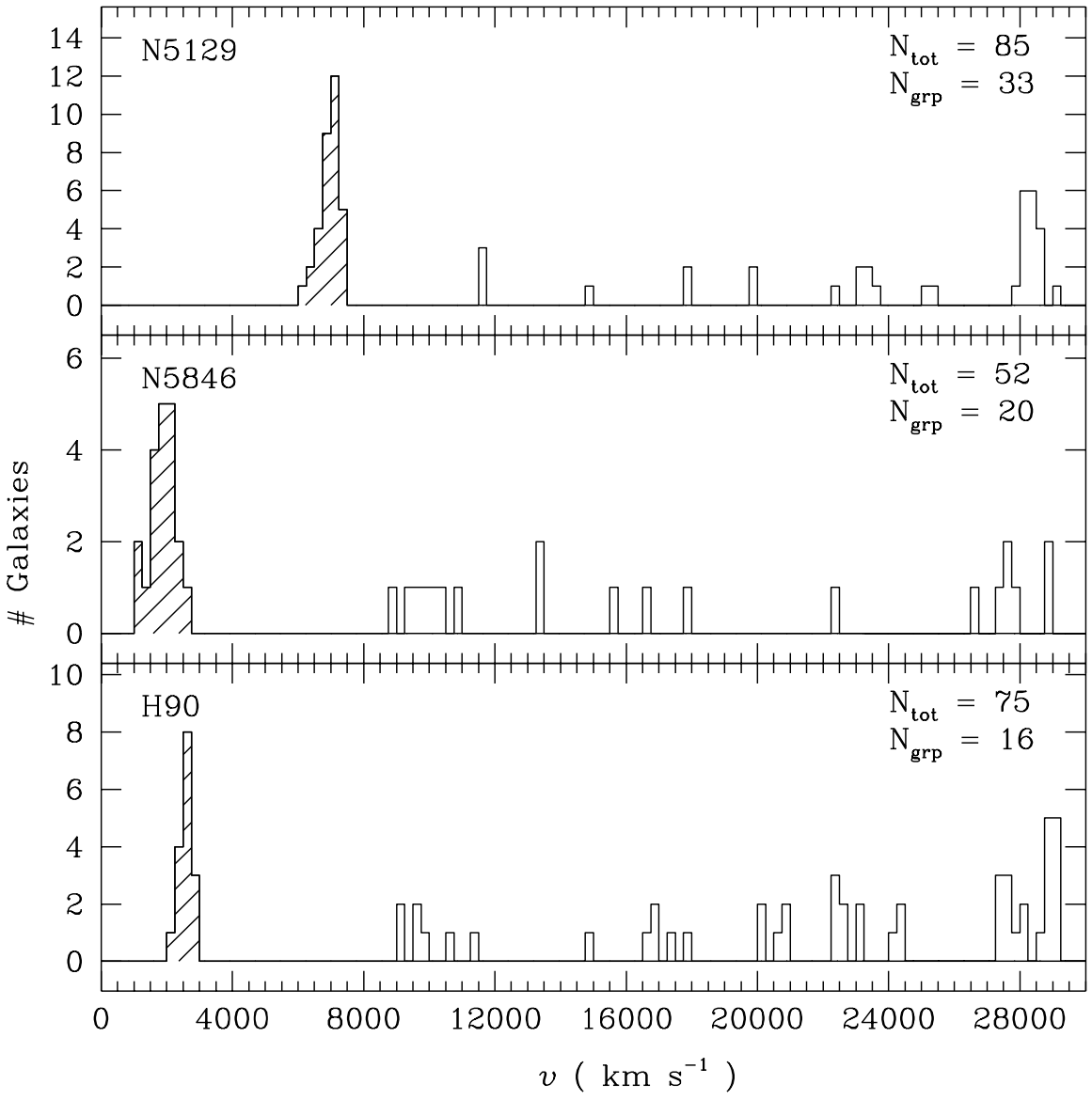
N5129
N_tot = 85
N_grp = 33
N5846
N_tot = 52
N_grp = 20
H90
N_tot = 75
N_grp = 16
# Galaxies
v (km s^-1)
0
4000
8000
12000
16000
20000
24000
28000

Fig. 2.— *cont.*

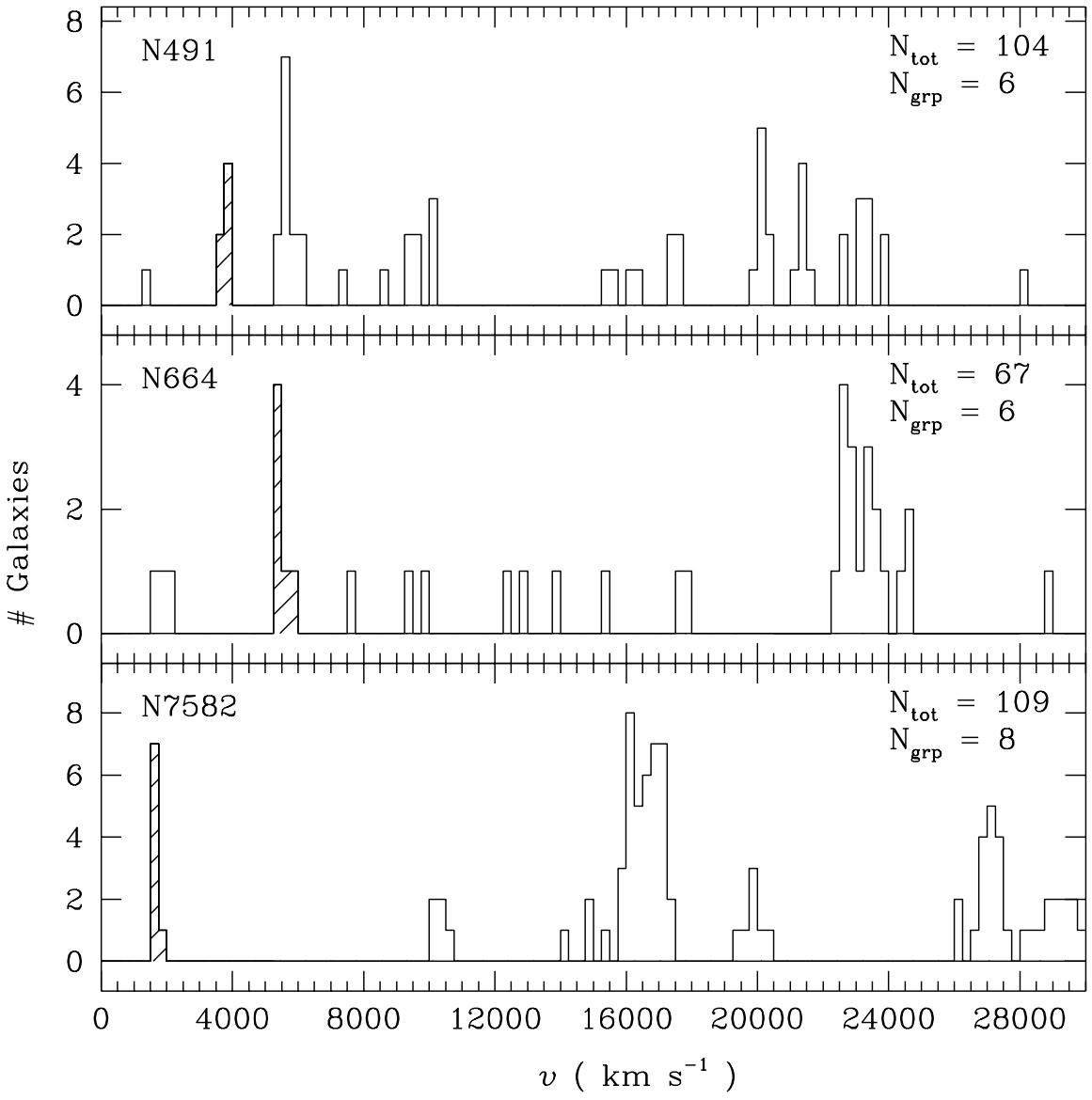
N491
N_tot = 104
N_grp = 6
N664
N_tot = 67
N_grp = 6
N7582
N_tot = 109
N_grp = 8
# Galaxies
v (km s^-1)
0
4000
8000
12000
16000
20000
24000
28000

Fig. 2.— *cont.*

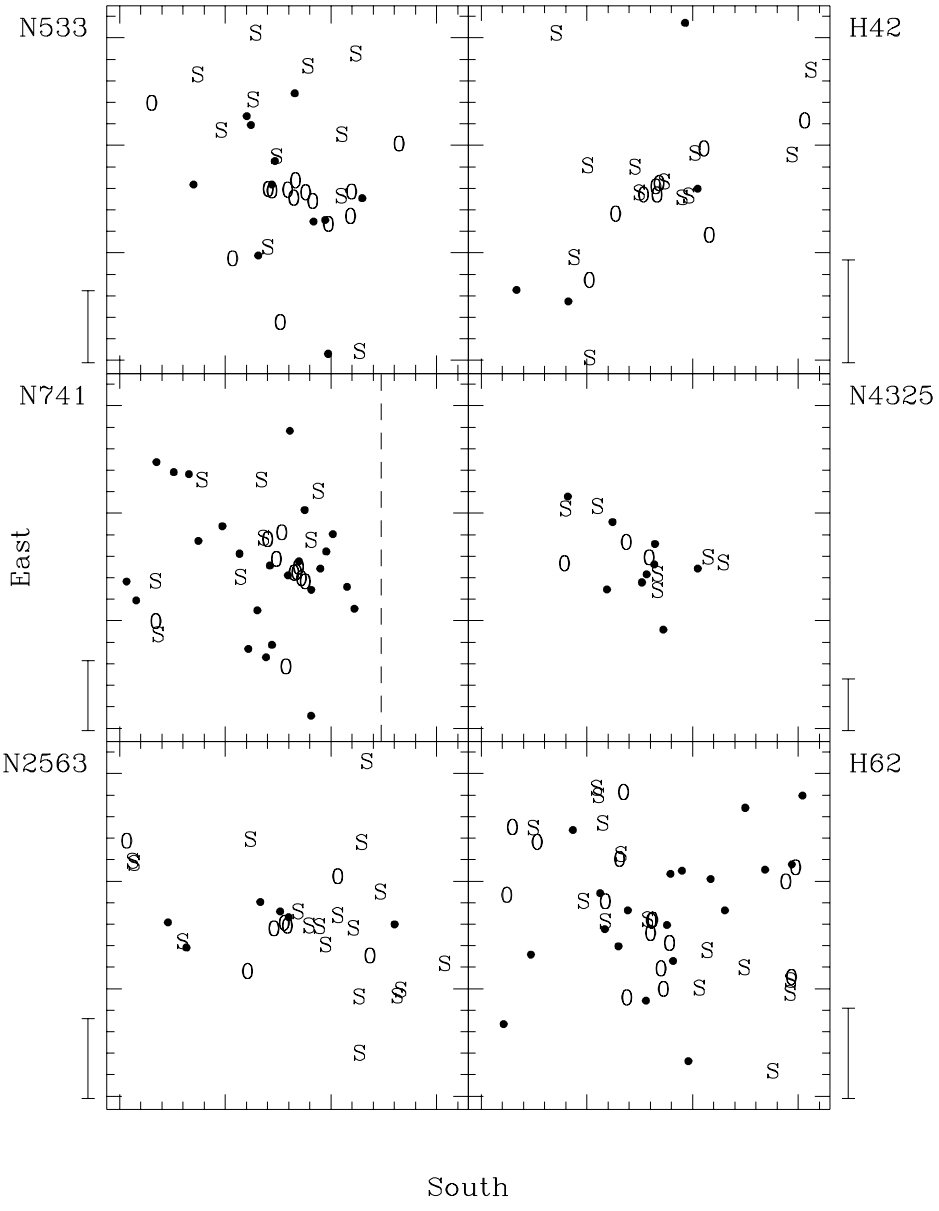

Fig. 3.—

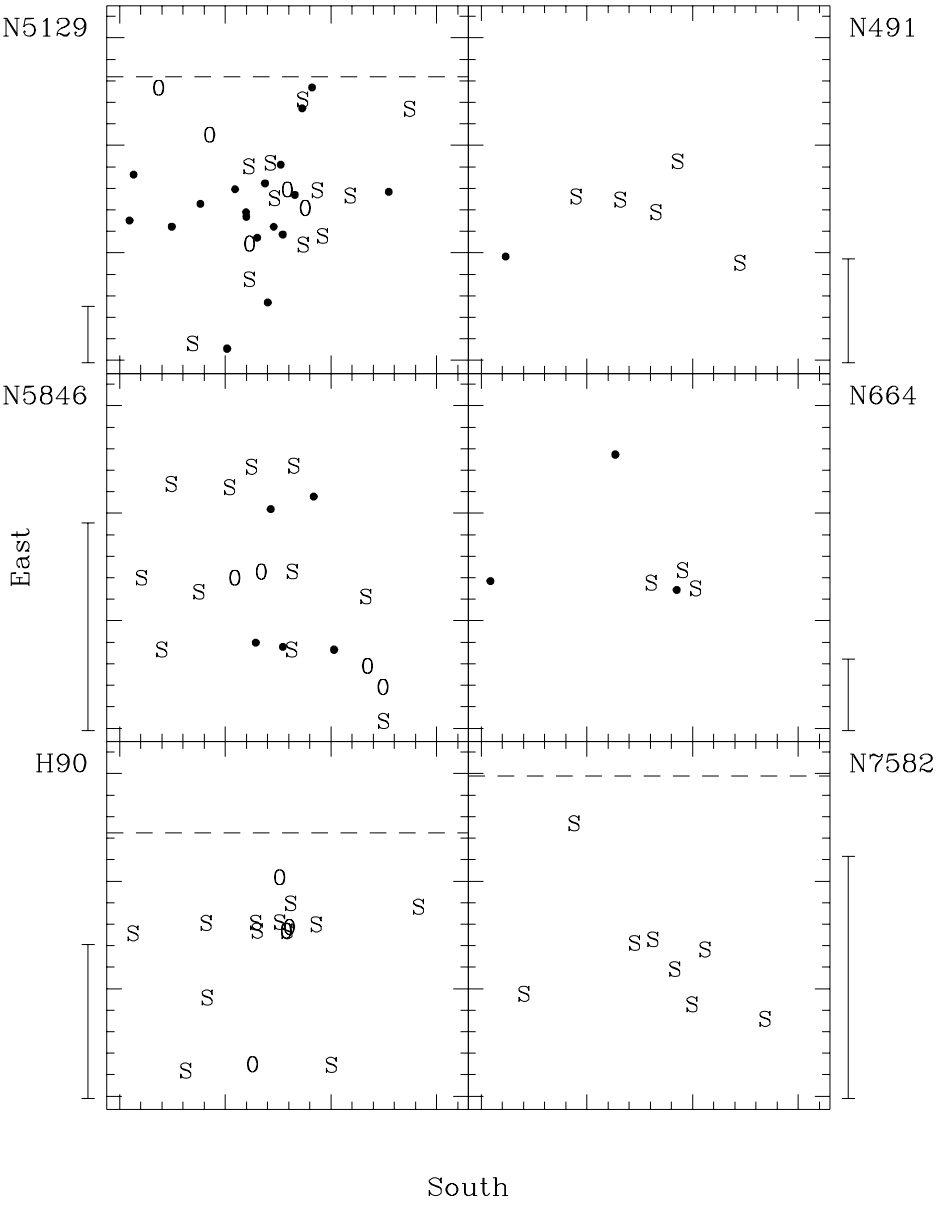

Fig. 3.— *cont.*

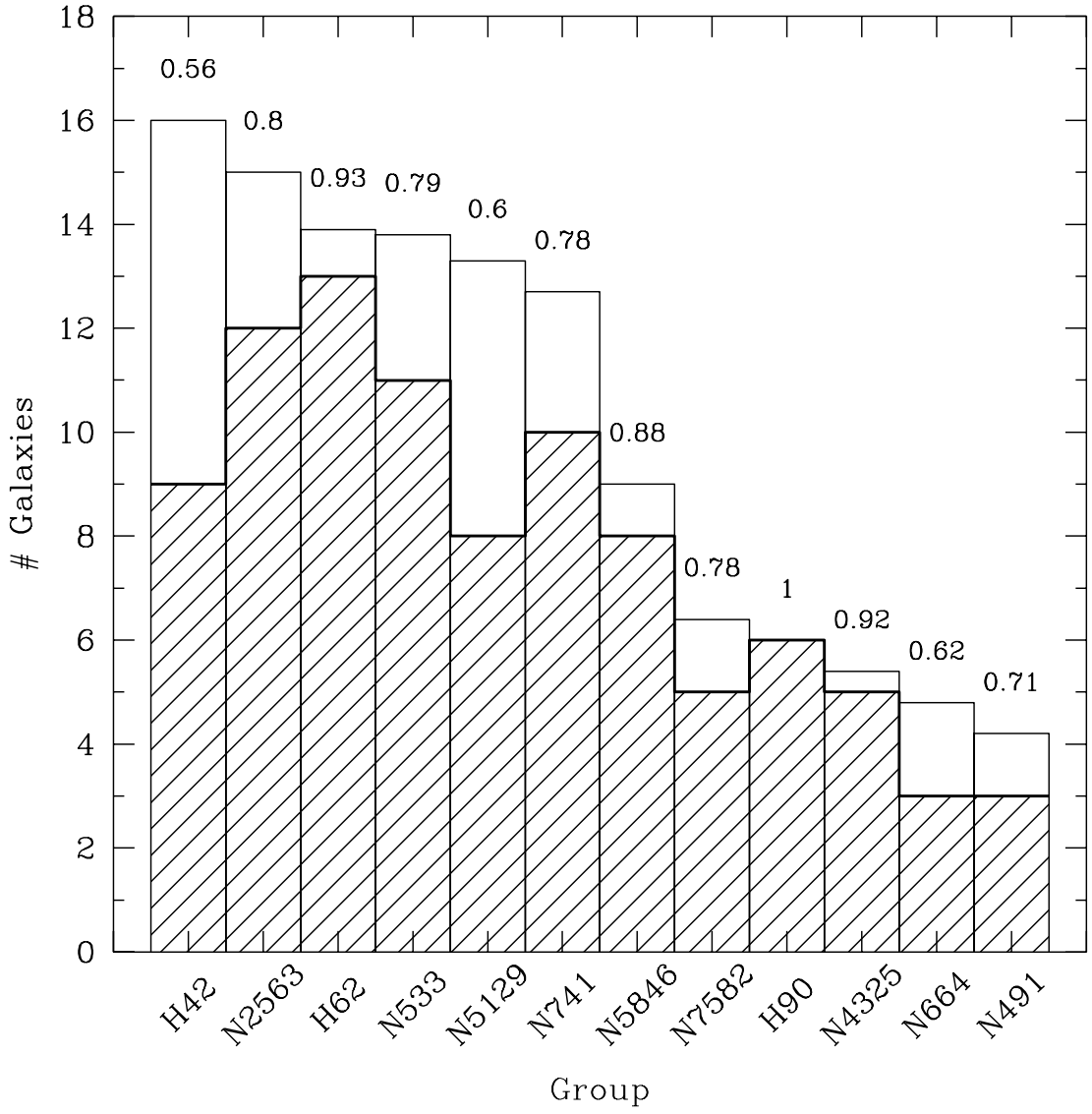
18
16
14
12
10
8
6
4
2
0
Galaxies
0.56
0.8
0.93
0.79
0.6
0.78
0.88
0.78
1
0.92
0.62
0.71
H42
N2563
H62
N533
N5129
N741
N5846
N7582
H90
N4325
N664
N491
Group

Fig. 4.—

Fig. 5.—

Fig. 6.—

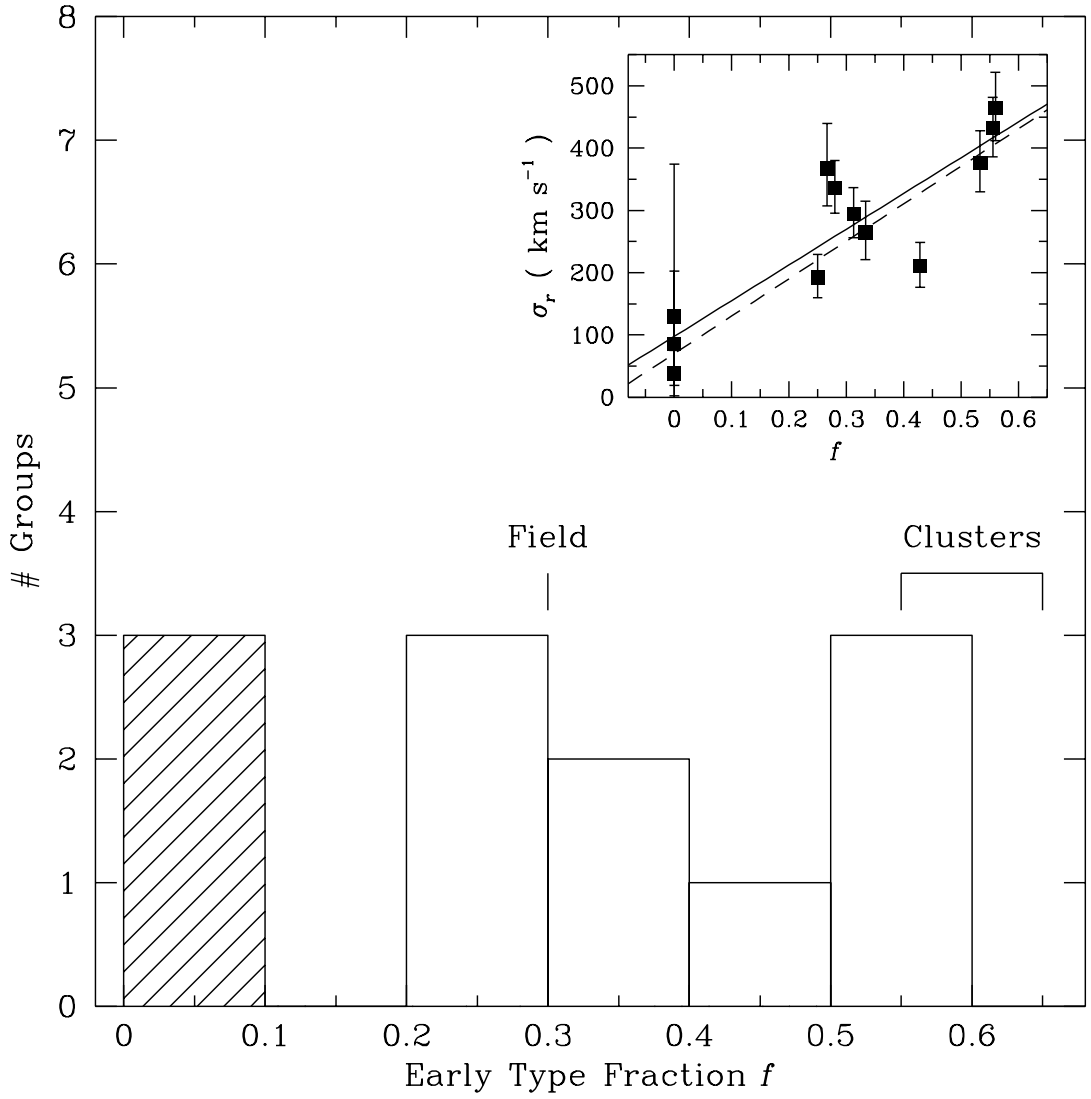
8
7
6
5
4
3
2
1
0
Groups
Field
Clusters
0
0.1
0.2
0.3
0.4
0.5
0.6
Early Type Fraction f
500
400
300
200
100
0
σ_r (km s^{-1})
0
0.1
0.2
0.3
0.4
0.5
0.6
f

Fig. 7.—

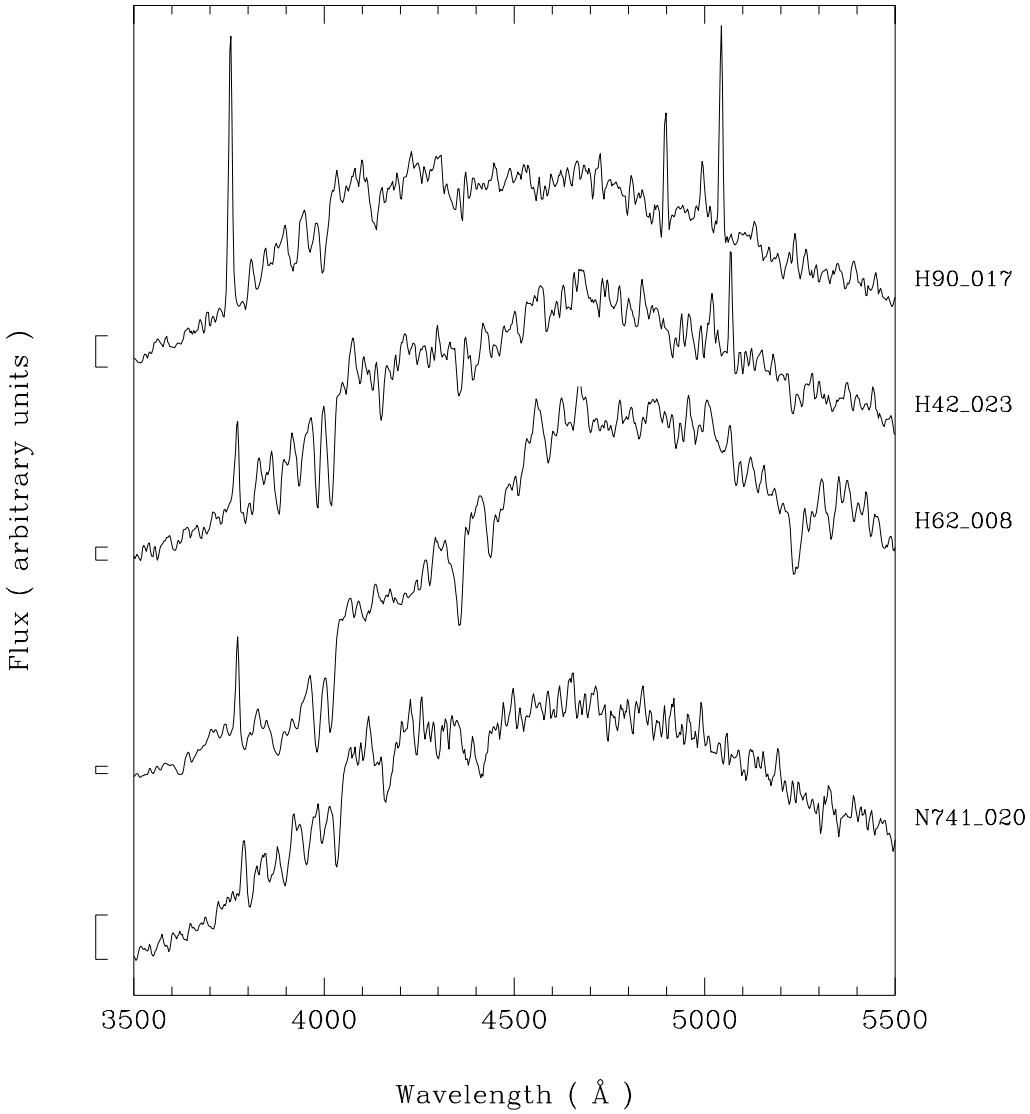
H90_017
H42_023
H62_008
N741_020
Flux (arbitrary units)
3500
4000
4500
5000
5500
Wavelength (Å)

Fig. 8.—

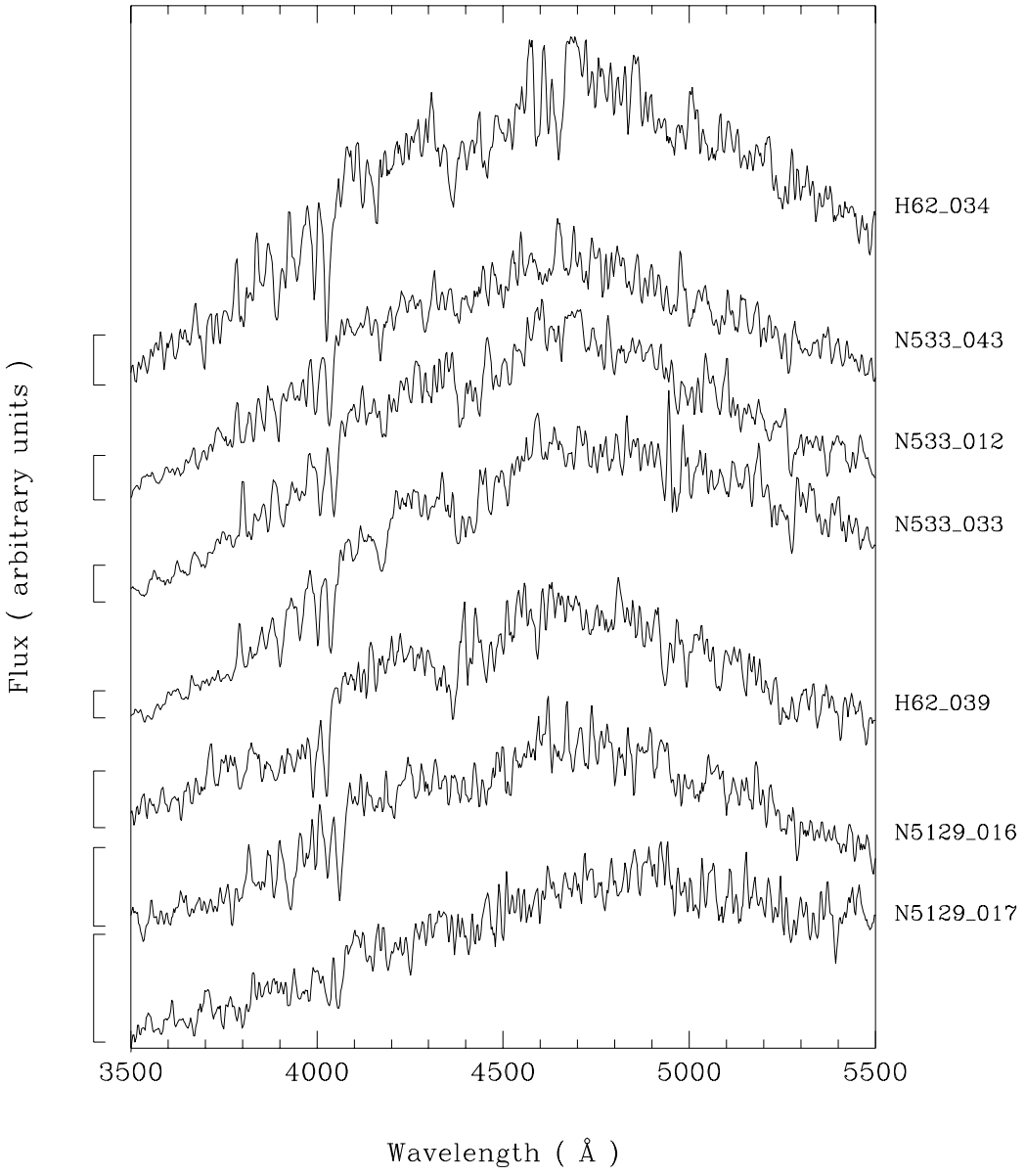
H62_034
N533_043
N533_012
N533_033
H62_039
N5129_016
N5129_017
Flux (arbitrary units)
3500
4000
4500
5000
5500
Wavelength (Å)

Fig. 8.— *cont.*

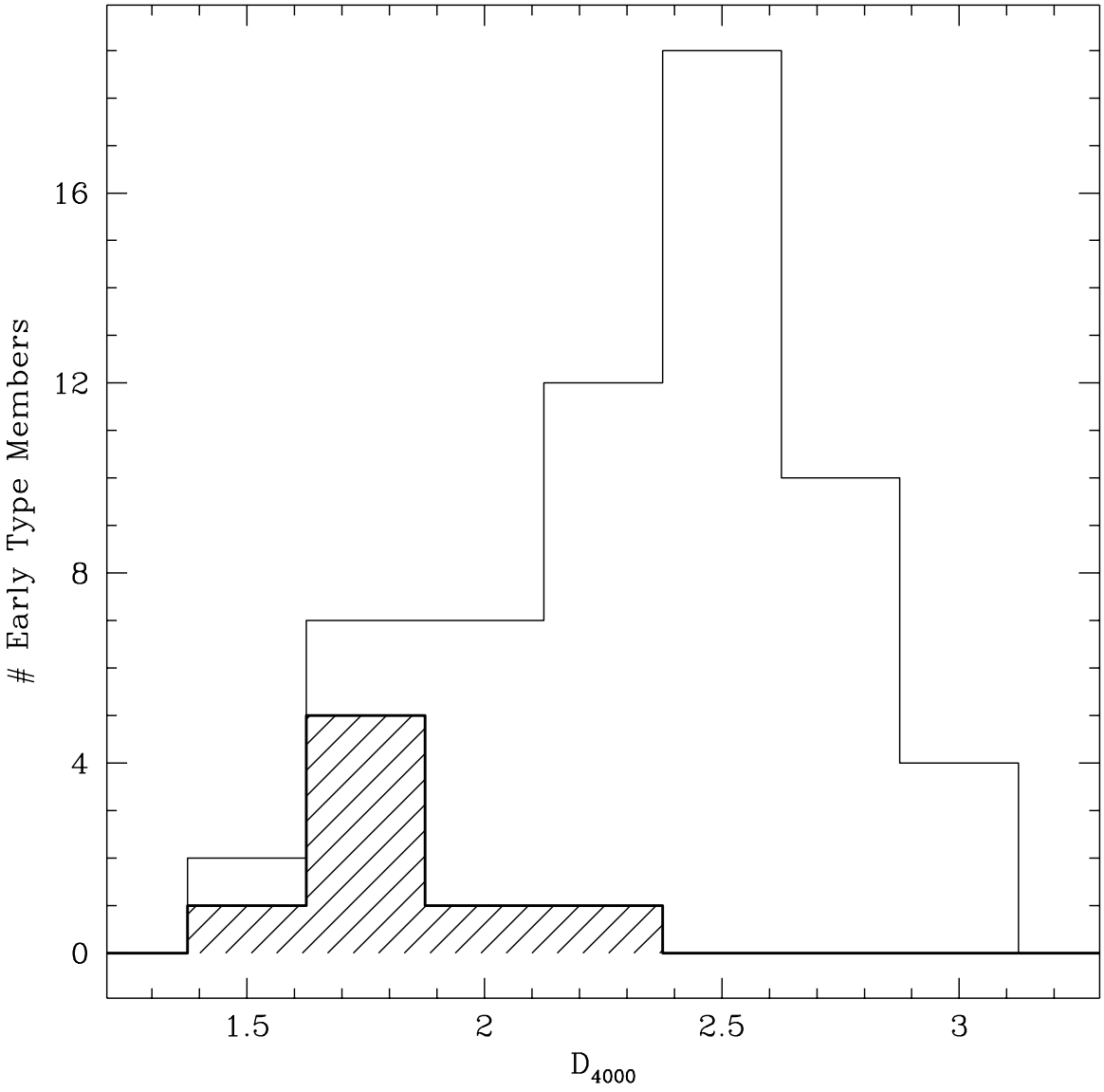

Fig. 9.—